Prokaryotic, Microeukaryotic, and Fungal Composition in a Long-Term Polychlorinated Biphenyl-Contaminated Brownfield

Flavien Maucourt, Aurélie Cébron, Hélène Budzinski, Karyn Le Menach, Laurent Peluhet, Sonia Czarnes, Delphine Melayah, David Chapulliot, Laurent Vallon, Gaël Plassart, et al.

Prokaryotic, microeukaryotic and fungal composition in a long-term polychlorinated biphenyl-contaminated brownfield

Flavien Maucourt[1], Aurélie Cébron[2], Hélène Budzinski[3], Karyn Le Menach[3], Laurent Peluhet[3], Sonia Czarnes[1], Delphine Melayah[1], David Chapulliot[1], Laurent Vallon[1], Gaël Plassart[4], Mylène Hugoni[1,5a], Laurence Fraissinet-Tachet[1a]*

[1] *Univ Lyon, Université Claude Bernard Lyon 1, CNRS, INRAE, VetAgro Sup, UMR Ecologie Microbienne, Villeurbanne, F-69622 France*

[2] *Université de Lorraine, CNRS, LIEC, Nancy F-54000, France*

[3] *Université de Bordeaux, CNRS, EPOC, Bordeaux F-33405, France*

[4] *ENVISOL, 2-4 rue Hector Berlioz, La Tour du Pin F-38110, France*

[5] *Institut Universitaire de France (IUF)*

[a] *Contributed equally to this work*

Current address for M. Hugoni and D. Melayah: Univ Lyon, INSA Lyon, CNRS, UMR 5240 Microbiologie Adaptation et Pathogénie, F-69621 Villeurbanne, France

Corresponding author: Laurence Fraissinet-Tachet – laurence.fraissinet-tachet@univ-lyon1.fr

Authors ORCID:

Laurence Fraissinet-Tachet: 0000-0003-0073-8761

Mylène Hugoni: 0000-0002-2430-1057

Maucourt Flavien : 0000-0002-8030-5394

Keywords: polychlorinated biphenyls, metabarcoding, microbial communities, brownfield, soil, pollution

Running title: Microbial diversity into a PCB-contaminated soil

1 Abstract

Polychlorinated biphenyls (PCBs) are recognized as persistent organic pollutants, and accumulate in organisms, soils, waters, and sediments, causing major health and ecological perturbations. Literature reported PCB bio-transformation by fungi and bacteria *in vitro*, but data about the *in situ* impact of those compounds on microbial communities remained scarce while being useful to guide biotransformation assays. The present work investigated for the first time microbial diversity from the three-domains-of-life in a long-term contaminated brownfield (a former factory land). Soil samples were ranked according to their PCB concentrations and a significant increase in abundance was shown according to increased concentrations. Microbial communities structure showed a segregation from the least to the most PCB-polluted samples. Among the identified microorganisms, *Bacteria* belonging to *Gammaproteobacteria* class, as well as *Fungi* affiliated to *Saccharomycetes* class or *Pleurotaceae* family, including some species known to transform some PCBs were abundantly retrieved in the highly polluted soil samples.

2 Introduction

Microbial diversity is crucial for soil ecosystem functioning and ecosystemic services they deliver [1]. In the last centuries, human activities have broadly altered soil quality and functioning, including micro-organisms, by using toxic compounds known as xenobiotics. Among those xenobiotics, persistent organic pollutants (POPs) are of major health and ecological concerns as many bioaccumulated and biomagnified in the trophic network [2]. According to the Stockholm Convention from 2001, POPs included the class of polychlorinated biphenyls (PCBs) consisting in poly-chlorinated aromatic compounds (209 theoretical chlorinated forms named congeners and 150 physically synthesizable forms), used in the industry from 1929 to their prohibition at the end of 1980s as they were recognized as endocrine disruptors and carcinogenic substances [3, 4]. Presently, those molecules are still recovered in organisms as well as in ecosystems, from soils to waters and sediments. PCB soil decontamination

represents a challenge for management and restoration policies of impacted sites and mostly involves physico-chemical methods which are expensive, long and often generating by-products like furans or dioxins, also known as carcinogenic molecules [5]. A recent costless alternative, consisting in bioremediation (*i.e.* process used to treat contaminated media by living organisms) emerged from several studies highlighting the capacity of microorganisms to transform some PCB molecules [6, 7].

Most studies focusing on bacterial and fungal PCB transformation were conducted *in vitro* [7–9] but recent bioremediation and rhizoremediation studies of PCB contaminated sites have been reported supporting that bioremediation is a promising way to depollute PCBs [10–13]. Those previous works showed the ability of microorganisms affiliated mainly with *Proteobacteria, Actinobacteria, Firmicutes, Chloroflexi, Dehalococcoides* and the white rot *Fungi* functional guild to transform PCBs [6, 14, 15]. Other non-lignolytic *Ascomycota* fungi were also reported as PCB transformers such as *Purpureocillium lilacinus* [16]. Because of their hyphal structure, all these filamentous fungi are suggested as good candidates to easily penetrate polluted matrices and access to poorly bio-accessible pollutants [17]. Those filamentous fungi can also act as dispersion vector of bacteria [17] even if bacteria already have good reported dispersal capabilities [18]. These in vitro studies mostly analyzed the transformation of few PCBs suggesting that their depollution action with respect to all PCBs congeners is finally quite partial. Moreover, the actual limit of *in vitro* PCB transformation studies is the lack of cultured microbial representatives. In contrast, *in situ* studies are still scarce and few characterized the cultivable fraction of *Fungi* retrieved in PCB-polluted-soils. Previous works showed the presence of *Acremonium, Aspergillus, Paecilomyces, Penicillium, Phomopsis, Cladosporium, Doratomyces, Myceliophtora* by using cultivation methods [8, 19–21]. By using 454 pyrosequencing, more recent *in situ* studies identified *Proteobacteria, Actinobacteria, Firmicutes* and *Basidiomycota* phyla, including species already known to transform PCBs (Stella *et al.*, 2017; Zenteno-Rojas *et al.*, 2020). Other studies also reported that PCB

contamination increased soil fungal richness and promoted the development of bacterial species able to metabolize these pollutants [24, 25]. But among these studies focusing on microbial diversity under PCB contaminated ecosystems, none investigated micro-eukaryotes (other than *Fungi*) neither archaeal diversity. Moreover, soil *in situ* studies are still scarce while they represent the better way to fully assess microbial diversity that could be involved in PCB transformation at the ecosystemic level.

We hypothesized that in long term PCB contaminated soils, pollution impact microorganisms composition from the three-domains-of-life and select those adapted and potentially involved in transformation of some PCBs. In the present work, we aimed at testing if microbial abundance and composition from the three-domains-of-life differ in contrasted PCB concentrations to identify PCB tolerant microorganisms including some possibly involved into PCB transformation. This work took advantage of a brownfield (a formerly factory land) that presented a spatially heterogeneous PCB exposition.

3 Experimental Procedures

3.1 Study site, sampling, and PCB concentrations

Soil, whose characteristics were detailed into the supplementary experimental procedures, was sampled in a peri-urban site in Pont-de-Claix, Isère, France (45,136578°N 5,697205°E). This site is a brownfield where a painting factory was established in 1956, demolished and forsaken since 2009. In 2017, engineering consultants from ENVISOL (www.envisol.net) transformed this brownfield (contaminated by PCBs for more than six decades) into an experimental site for the research and innovation CRISALID project in field of sustainable development and brownfield depollution (Centre de Réflexion ISérois en Aménagement Durable, IDfriches: http://www.crisalid-idfriches.fr). On October the 15th 2018, twenty soil cores were randomly sampled, on a sampling grid with samples separated by at least 4 meters apart

from two different geographical areas on the brownfield, called “Zone 2” and “Zone 3/4” corresponding to paint storage and production areas respectively. Briefly, for each sample, 500 g of soil was taken out, from 0 to 10 cm depth with 12-cm diameter, sieved (2-mm), homogenized manually and stored at -80°C in 50 g portions until nucleic acid extraction and PCB chemical assay of 71 congeners as described in supplementary text. Complementarily, for each sample, 375 g of sieved-soil stored few days at 4°C have been directly used for indicator PCB (iPCB) assay according to GC/MS/MS method [Hexane / Acetone exctract] – NF EN 16167 – XP X 33-012 method (Eurofins).

3.2 C-CO_2 Microbial mineralization and enzymatic biological activity assay

For microbial mineralization, ten grams of dry weight soil, adjusted to 60% soil water retention capacity (WRC), were incubated at 24°C into 150 ml glass flasks hermetically sealed. A 3-mL portion of the flask atmosphere was sampled with a syringe and analyzed for CO_2 content through infrared spectrophotometer (Binos 1004) [26]. Microbial activity was evaluated using fluorescein diacetate (FDA) as a substrate on soil samples in triplicates at the SEMSE laboratory (https://www.semse.fr) according to a protocol derived from Schnürer & Rosswall (1982) [27]. Experimental details were developed into the supplementary text.

3.3 DNA extraction and Illumina sequencing

Three DNA extractions were conducted from 2 g of soil for each sample, pooled and quantified by Nanodrop (ND 1000 S Spectrophotometer®). A first step allowing protein removal was conducted using phenol/chloroform/isoamyl alcohol (25/24/1) using the Power Soil DNA Isolation kit according to the manufacturer recommendation (Mo Bio Laboratories, Carlsbad, CA, USA). Additionally, a DNA extraction was carried out without any biological matrix, quantified, and considered as a negative control to evaluate eventual ambient contaminations. Quality was verified by 1% agarose gel electrophoresis. For sequencing, PCR were performed, in triplicates, on a Biorad C1000 thermal cycler (Biorad), using:

0.5 U of Taq DNA polymerase (Invitrogen, Illkirch, France), 1X PCR Buffer, 1.5 mM of $MgCl_2$, 0.8 µM of each primer, 0.2 mM of each dNTP, 8 µg of BSA (New England Biolabs) and 20 ng of soil metagenomic DNA, in a final volume of 25 µL. The PCR programs, for the 16S and 18S rRNA amplifications, were both composed of 10 min at 94°C, 35 cycles of 1 min at 94 °C, 1 min at 58°C, and 1 min 30 sec at 72 °C, followed by 10 min at 72°C.For fungal ITS amplification, PCR conditions used were 3 min at 94 °C, 35 cycles of 45 s at 94°C, 45 s at 50°C, and 45 s at 72 °C, followed by 7 min at 72°C.The three PCR replicates from each sample were pooled, purified with Agencourt AMPure XP PCR Purification kit (Beckman Coulter, Villepinte, France), and quantified using the Quant-iT Picogreen dsDNA Assay Kit (Life Technologies, NY, USA). Prokaryotic amplification of the V3-V5 region of the 16S rRNA genes was performed using the universal primers 515F (5'- α-GTG-YCA-GCM-GCC-GCG-GTA -3' [28]) and 909R (5'- β-CCC-CGY-CAA-TTC-MTT-TRA-GT -3' [29]). Eukaryotic amplification of the V4 region of the 18S rRNA genes was performed using the universal primers TAReuk_F (5'-α-CCA-GCA-SCY-GCG-GTA-ATT-CC -3') and TAReuk_R (5'-β-ACT-TTC-GTT-CTT-GAT-YRA -3') [30]. Fungal amplification of the ITS-2 region was conducted using the primers fITS7 (5'- α-GTG-YCA-GCM-GCC-GCG-GGT-A-3') and ITS4 (5'- β-TCC-TCC-GCT-TAT-TGA-TAT-GC-3') [31]. For all primer sets, α and β represented the two Illumina overhanging adapter sequences (TCG TCG GCA GCG TCA GAT GTG TAT AAG AGA CAG and GTC TCG TGG GCT CGG AGA TGT GTA TAA GAG ACA G, for α and β, respectively) allowing the construction of amplicon libraries by a two-step PCR. Amplicons libraries production was produced on the Illumina MiSeq platform (2 x 250-bp paired-end reads) by Biofidal, Vaulx-en-Velin, France - http://www.biofidal-lab.com.

3.4 Sequence processing

Prokaryotic 16S rRNA gene, eukaryotic 18S rRNA gene and ITS paired-end reads were merged with a maximum of 10% mismatches in the overlap region using Vsearch [32]. Additional denoising procedures consisted in discarding reads either with no expected length (i.e. expected size between 250 to 580 bp, 250 to 450 bp, 200 to 600 bp for prokaryotic 16S rRNA genes, eukaryotic 18S rRNA genes and ITS regions, respectively) or containing ambiguous bases (N). After dereplication, the clusterisation tool ran with SWARM [33] that used a local clustering threshold. In the present work, the aggregation distance equals 3. Chimeras were then removed using Vsearch and low abundance sequences were filtered at 0.005%, i.e. Operational Taxonomic Units (OTUs) with at least 0.005% of all sequences were kept [34]. Taxonomic affiliation was performed with both RDP Classifier [35] and Blastn+ [36] against the 132 SILVA database [37] for 16S and 18S rRNA genes and the ITS region. This procedure was automated in the FROGS pipeline [38]. Then, a normalization procedure was applied to compare samples and the datasets were randomly resampled down to 5,544 sequences for prokaryotic marker, to 6,845 sequences for 18S rRNA amplicons and to 12,407 for ITS region.

3.5 Statistical analyses

A dissimilarity coefficient was measured between samples depending on total PCB contamination, using the Gower method (quantitative and symmetric [39]). Then, applying the distance matrix (function *vegdist*, in R package *vegan* [40]), samples were grouped according to their PCB concentration by Ward method (function *hclust*, in R package *stat* [41]). A dendrogram was built using the *ggdendro* package in R and *ggplot2* [42]. Richness (Chao1) and diversity (Shannon) indices were computed with Past3 program [43]. The comparison of richness and diversity indices for each polluted group was conducted by a Wilcoxon test (function *wilcox.test* in R package *stat*) as the mean comparison of number of DNA sequences copies obtained by qPCR method. An ordination of the samples using NMDS approach at

OTU level on Bray-Curtis dissimilarity matrices was performed (function *metaMDS* in R package *vegan*) and a stress value was calculated to measure the difference between the ranks on the ordination configuration and the ranks in the original similarity matrix for each repetition [44]. An acceptable stress value should be below 0.1. The difference between P0 group, considered as the non-polluted group, and P1,P2,P3 and P4 polluted groups was tested using PERMANOVA analysis on Bray-Curtis dissimilarity matrices using the *adonis* function from the package *vegan*. To analyze common and/or specific OTUs according to the different groups, Venn diagram was realized with the online tool Ugent (http://bioinformatics.psb.ugent.be/webtools/Venn/). Heat-maps were generated with the *Phyloseq* package coupled with the *ggplot* and *vegan* packages in the R software.

3.6 **Quantitative PCR**

qPCR analyses were performed on a CFX96 Touch Real-Time PCR System (Bio-Rad) running CFX Maestro Software 2.0 using the same primers that the ones used for metabarcoding assay without the Illumina overhanging adapter sequences. Copy numbers of 16S rRNA genes, 18S rRNA genes and ITS regions in the environmental DNA samples were determined in duplicate on the non-diluted sample and for two different sample dilutions (10-fold and 100-fold). The reaction mixture (20 µL) contained SensiFAST™ SYBR® No-ROX Kit. For a 20 µL reaction mix, 20 µM of primers and ultra-pure sterile water were added. All reactions were performed in 96-well qPCRplates (Eurogentec) with optical tape (Eurogentec). Two microliter of diluted (10-fold and 100-fold) or non-diluted environmental DNA was added to 18 µl of mix in each well. The accumulation of newly amplified double-stranded gene products was followed online as the increase in fluorescence due to binding of SYBR Green fluorescent dye. All qPCR programs are listed in Table S4. The fluorescence signal was read in each cycle after the amplification step to ensure stringent product quantification. Specificity for the qPCR reaction was tested by melting curve analysis (65°C-97°C) and then by electrophoresis on 1% agarose gel. Standard curves

for the targeted genes (16S rRNA gene,18S rRNA gene and ITS region) were generated from a mix of plasmids representative of the environment studied. Next, serial dilutions of previously titrated suspensions were performed and amplified by conventional PCR from environmental clones and then purified (NucleoSpin® Plasmid, Macherey-Nagel) and quantified for this study. All reactions were performed with standard curves spanning from 10^1 to 10^8 copies of targeted gene per mL. Mean PCR efficiencies and correlation coefficients for standard curves were as follows: for the 16S rRNA gene assay, 91.71 %, $r^2 = 0.99$, for the 18S rRNA gene assay, 81.95 %, $r^2 = 0.99$, and for the ITS region assay, 90.92 %, $r^2 = 0.99$.

4 Results

4.1 PCB concentration analyses and soil sample clustering

Physico-chemical characteristics of the sample site, localized in Pont de Claix (France), are listed in Table S1, and described an alkaline soil with heterogeneous texture. The twenty soil samples, randomly collected, displayed variable indicator PCB (iPCB) concentrations from 0.03 to 31.11 mg. kg^{-1} dry mass of soil (Table 1). Some samples presented low iPCB concentrations (between 0.03 and 0.51 mg.kg^{-1} dry mass of soil) while other soil samples were characterized by a higher level of iPCBs (from 1.67 to 31.11 mg.kg^{-1} dry mass of soil). Among the iPCBs detected in this site, the PCBs 28, 52, 101, 118, 138, 153 and 180 represented 10, 32, 18, 15, 10, 10 and 5% of the total iPCBs respectively, the higher chlorinated iPCB 180 being the less abundant congener. Complementarily, 71 supplemental PCBs (including the 7 iPCBs) were assayed directly in soil ranging from 0.61 to 135.84 mg.kg^{-1} dry mass of soil (Table S2). Globally, the total concentration of the 71 PCBs was proportional to the total concentration of iPCBs confirming that iPCBs were reliable PCB indicators in this site. Consequently, further analyzes were conducted considering only the iPCB concentration of each sample as a *proxy* of soil contamination level.

A hierarchical clustering of samples was performed according to iPCB concentrations showing a segregation of the samples (Figure 1A). Three groups, named P0, P1 and P2, were represented by 5 or 6 soil samples and two other groups, named P3, contained only two samples, and P4 that regrouped the two last most PCB concentrated samples. The P0 group was characterized by the lowest iPCB concentrations from 0.03 to 0.51 $mg.kg^{-1}$ dry mass of soil and considered as the non-polluted group related to the threshold of 1 $mg.kg^{-1}$ established by the local decision making. P1 group contained iPCB concentrations from 1.67 to 3.83 $mg.kg^{-1}$, P2 from 4.66 to 7.69 $mg.kg^{-1}$, P3 from 10.06 to 14 $mg.kg^{-1}$ and P4 from 21.60 to 31.11 $mg.kg^{-1}$.

4.2 Structure of microbial communities in PCB contaminated soils

This work investigated the changes in prokaryotic, microeukaryotic and fungal community structure in the soil samples presenting a PCB gradient. Normalized datasets consisted in 1477 prokaryotic OTUs (representing 99,792 quality-filtered paired-end sequences and 388 to 795 OTUs per sample); 752 microeukaryotic OTUs (representing 116,365 sequences and 199 to 339 OTUs per sample); and 685 fungal OTUs (representing 248,140 sequences and 113 to 313 OTUs per sample) (Table S3). Rarefaction curves indicated that some samples almost reached an asymptote in the prokaryotic dataset (Figure S1A) and that the sequencing effort was sufficient to describe microeukaryotic and fungal diversity (Figure S1B and C).

The difference in prokaryotic, microeukaryotic and fungal OTUs composition, assessed through a permutation analysis of variance (PERMANOVA), showed significant differences for P0 group compared to the other groups P1, P2, P3 and P4 for prokaryotes (p=0.002, R=0.31) while only trends were detected for microeukaryotic (p=0.072, R=0.25) and fungal communities (p=0.069, R=0.39). Moreover, the NMDS, realized at OTU level, graphically showed a segregation between the P0 group

on the first hand and the P1, P2, P3 and P4 groups on the other hand, especially for the prokaryotic dataset and supported with stress values of 0.099, 0.075 and 0.080 (Figure 1B, 1C and 1D), respectively.

The prokaryotic richness (estimated through the Chao1 index) of the P0 group was significantly lower compared to P1 group (p = 0.05) (Figure S2A). The same trend was observed for the microeukaryotic richness with a marginal significance (p = 0.06) between P0 and P1 groups, being significant between P0 and P2 groups (p = 0.02, Figure S2B). No significant differences were observed for Chao1 richness based on the fungal marker (Figure S2C). Prokaryotic diversity (estimated through the Shannon index) (Figure S2A) was significantly lower in P0 group compared to P1 group (p = 0.01) and P2 group (p = 0.03) and the same trend was observed between P0 and P3 groups, being marginally significant (p = 0.09) whereas microeukaryotic and fungal diversity was not significantly different whatever the PCB contamination level (Figure S2B and C).

4.3 Prokaryotic community composition

The present work showed a predominance of *Bacteria* over *Archaea* and the later representing less than 1% of the total prokaryotic sequences and mainly affiliated with *Thaumarchaeota*. The detailed analysis of bacterial composition showed that *Acidobacteria*, *Actinobacteria* and *Proteobacteria* were the most abundant phyla, representing 225, 318, 485 OTUs (17.76%, 25.51% and 33.71% of the total sequences), respectively (Figure 2A). *Actinobacteria* and *Chloroflexi* showed lower abundance from P0 to P4 (from 34.06% and 4.11% to 18.28% and 1.40% of the total sequences, respectively) contrary to *Proteobacteria* phylum with higher abundance in P4 than P0 (from 41.62% to 20.88% of the total sequences). At the class taxonomic level, the *0319-7L14*, *MB-A2-108* (both from *Actinobacteria*), *P2-11E* (*Chloroflexi*) soil groups and *Oxyphotobacteria* (*Cyanobacteria*) were enriched in P0 group. *Gitt-GS-136* soil group from *Chloroflexi* was only enriched in P0 and P1. *Thermoleophilia* (*Actinobacteria*) and *Gemmatimonadetes* (*Gemmatimonadetes*) showed a decreasing abundance from P0 to P4 (from 8.64% and 10.87% to 2.80%

and 4.37% of the total sequences, respectively). Conversely, *Longimicrobia* (*Gemmatimonadetes*) class was only detected in P4 group and the *Gammaproteobacteria (Proteobacteria)* showed an increasing abundance from P0 to P4 (11.23% to 30.21% of the total sequences). In the same way, *Deltaproteobacteria (Proteobacteria)* showed a rising abundance from P0 to P3 (11.23% to 30.21% of the total sequences) but its abundance decreased in P4 group.

At the family taxonomic level (Figure 2B), the *Nocardioidaceae*, three unknown families from *Gaiellales* and *IMCC26256* order and *0319-7L14* class (all belonging to *Actinobacteria*) and the *Rhodobacteracea* family (*Proteobacteria*) were enriched in the P0 group. Some families showed higher abundances in the P3 group specifically such as *bacteriap25* soil group, *Dongiaceae* and two unknown families from *RCP2-54* and *CCD24* classes (all belonging to *Proteobacteria*). Families only enriched in P4 group were *Xanthomonadaceae, Acidithiobacillaceae, Rhodanobacteraceae* (all belonging to *Proteobacteria*), *Microscillaceae* (*Bacteroidetes*), *Longimicrobiaceae* (*Gemmatimonadetes*) and an unknown belonging to *Subgroup7* (*Acidobacteria*).

4.4 **Microeukaryotic community composition**

At the phylum level (Figure 3A), the microeukaryotic composition showed decreasing abundance from P0 to P4 for *Cercozoa* and *Chytridiomycota* (from 32.73% and 15.74% to 25.04% and 5.58% of the total sequences, respectively) contrary to *Amoebozoa* with increasing abundance from P0 to P4 (3.41% to 11.37% of the total sequences). At the class taxonomic level, *Ulvophyceae* (*Chlorophyta*) and *Craspedida* (*Choanoflagellida*) classes were enriched in P0 and *Glissomonadida* (*Cercozoa*), *Chytridomycetes* (*Chytridiomycota*) and *Glomeromycetes* (*Glomeromycota*) showed a decreasing abundance from P0 to P4 (from 13.07%, 8.55% and 2.79% to 10.63%, 4.41% and 0% of the total sequences respectively). On the contrary, an unknown class belonging to *Charophyta* was enriched in P4 and *Arcellinida* and *Euamoebida* (both belonging to *Amoebozoa*) showed an increasing abundance from

P0 to P4 (2.24% and 1.16% to 3.99% and 7.37% of the total sequences respectively). In the same way, the *Intramacronucleata* class (*Ciliophora*) showed a rising abundance from P0 to P4 (6.49% to 24.51%) and specifically in P2 group (where it reached 40% of the total sequences).

At the family taxonomic level (Figure 3B), the microeukaryotic families enriched in the group P0 were *Mortierellaceae* (*Mortierellomycota*), *Glomeraceae* (*Glomeromycota*), *Spizellomycetaceae* (*Chytridiomycota*), two unknown families belonging to the *Troubouxiophycea* and *Chlorophyceae* classes (both belonging to *Chlorophyta*), two other belonging to *Glissomonadida* and an unknown class (both belonging to *Cercozoa*) and a last unknown family belonging to the *Craspedida* class (*Choanoflagellida*). One unknown family belonging to the *Vampyrellidae* class (*Cercozoa*) showed higher abundance in the P3 group. Families only enriched in P4 were *Colpodea*, *Nassophorea* (both belonging to *Ciliophora*), an unknow family from *Bdelloida* class (*Rotifera*) and a last unknown family belonging to *Charophyta*.

4.5 Fungal community composition

ITS dataset (Figure 4A) was dominated by *Ascomycota* and *Basidiomycota* representing 372 and 87 OTUs respectively, with 26.57 to 41.92% of *Ascomycota* and 23.15 to 28.99% of *Basidiomycota* in the different groups. The *Chytridiomycota* were detected with a small relative abundance whatever the groups with a decreasing abundance of sequences observed from P0 to P4 groups (from 12.43% to 4.27%, respectively). Fungal community analysis at the class level (Figure 4A) revealed that an unknown class (belonging to *Mortierellomycota*) only presented from the P2 to P4 groups (representing 8.07% to 9.08% of sequences). The *Saccharomycetes* class (belonging to *Ascomycota*) represented 7.93 and 4.54% of sequences only in P2 and P4 groups, respectively. An uncultured *Ascomycota* class was detected only in the P4 group representing 2.79% of sequences. The families *Aspergillaceae*, *Sporomiaceae*,

296 *Pleosporaceae, Pezizaceae* (all belonging to *Ascomycota*), *Powellomycetaceae* (*Chytridiomycota*),
297 *Tricholomataceae,* an unknown family from *Agaricales* (both belonging to *Basidiomycota*) presented a
298 higher abundance in P0 group (Figure 4B). The families *Halosphaeriaceae, Sympoventuriaceae* (both
299 belonging to *Ascomycota*), *Ceratobasidiaceae, Auriculariaceae, Psathyrellaceae* (all belonging to
300 *Basidiomycota*), two families from *Spyzellomycetales* and *Lobulomycetales* orders (*Chytridiomycota*)
301 were represented with a higher abundance in P3 group. The families *Plectosphaerellaceae,*
302 *Stachybotryaceae* (both from *Ascomycota*), *Pleurotaceae, Entolomataceae* and families from the orders
303 *Sebacinales* and *Agaricales* (all belonging to *Basidiomycota*) were represented by a drastic higher
304 abundance in the P4 groups and one family from *Saccharomycetales* (*Ascomycota*) was characterized by
305 a higher abundance in P2 and P4 groups.

306 ### 4.6 Core *versus* specific microbiome among PCB pollution

307 Common and specific OTUs among the five PCB concentration groups (P0 to P4) were investigated
308 using Venn diagrams. Common OTUs (or core OTUs) to the five groups consisted in 468 prokaryotic
309 OTUs (31.68% of prokaryotic richness), 157 microeukaryotic OTUs (20.87% of eukaryotic richness)
310 and 173 fungal OTUs (25.25% of fungal richness) (Figure S3, S4 and S5). Taxonomic information about
311 those common and specific OTUs were then analyzed at the family level considering only known families
312 (unknown families have been discarded from the bar diagram analysis). The most contaminated groups,
313 consisting in all combinations of P1 to P4 (P1+P2, or P1+P2+P3 or P3+P4 etc..), contained 25.42% of
314 the prokaryotic OTUs while less than 2.31% of the prokaryotic OTUs were specific to one group (P0,
315 P1, P2, P3 or P4) (Figure S3). Microeukaryotic communities harbored 1.23 to 4.52% of specific OTUs
316 to one group (P0, P1, P2, P3 or P4) (Figure S4). Concerning fungal OTUs, 1.02 to 4.49% of OTUs were
317 specific to one group (P0, P1, P2, P3 or P4) (Figure S5). Additional results were described in the
318 supplementary text.

4.7 Microbial abundance and activity

Prokaryotic, eukaryotic and fungal abundances were quantified using qPCR targeting the 16S rRNA gene, 18S rRNA gene and ITS region, respectively (Figure S6). An increase in microbial community abundance was observed from P0 to P1 and P2 as a trend for 16S rRNA genes and as statistically marginal or significant for 18S rRNA and fungal ITS from P0 to P1 (p = 0.08 for both), from P0 to P2 (p = 0.007 and 0.03, respectively), from P0 to P3 (p = 0.09 for both) and from P0 to P4 (p = 0.09 for both) (Figure S6). Indeed, prokaryotic 16S rRNA gene increased from $1.12x10^7$ copies per gram of soil on average in P0 while being on average $3.3x10^7$, $3.2\ 10^7$, $2.6x10^7$ and $2.7x10^7$ copies per gram of soil in P1, P2, P3 and P4, respectively. Eukaryotic abundance increased from $1.4x10^5$ 18S rRNA gene copies per gram of soil in P0 to $6.4x10^5$, $5.4x10^6$, $9.5x10^5$ and $7.9x10^5$ copies per gram of soil in P1, P2, P3 and P4, respectively. For the fungal community, abundance increased from $6.8x10^4$ copies per gram of soil in P0 to $3.3x10^5$, $6.0x10^6$, $4.6x10^5$ and $4.0x10^5$ copies per gram of soil in P1, P2, P3 and P4, respectively. These results agreed with: i) microbial mineralization assay (Figure S7A) that was significantly lower in the P0 group compared to the more polluted P4 one ($p\ value$ = 0.018), and; ii) microbial non-specific enzymatic FDA hydrolase activity assay (Figure S7B) that revealed an increase of global microbial enzymatic activities along the PCB pollution gradient.

5 Discussion

5.1 PCB effect on microbial abundance and activity

The studied site was heterogeneously contaminated by PCB indicating that pollution concentration was not location dependent. Literature reported other PCB polluted soils that presented heterogeneous pollution with PCB concentrations varying from 1 $mg.kg^{-1}$ dry mass [45] to over than 800 $mg.kg^{-1}$ dry

mass [25]. This ranked the Pont de Claix brownfield of this study as a "moderate" polluted site despite the weakly industrial painting production activity occurring in the past decades.

One key finding is that along the statistical ranking of PCB gradient in Pont de Claix samples, an increase of microbial activity, microbial abundance and diversity related to PCB concentrations was reported. This suggested that PCB might promote microbial growth and activity by providing carbon source or by generating a selection pressure leading resistant microbes to develop favorable coexistence.

The present work showed that prokaryotic communities were impacted by PCBs while microeukaryotic and fungal communities were impacted to a lesser extent but non-negligible. This impact on prokaryotic communities might be related to an accumulation of the well-known PCB dead-end intermediates named benzoate and chlorobenzoates [46] while some fungi are able to degrade this products [47]. Moreover PCB molecules seem to be not lethal for most of the eukaryotic communities (including fungal one), which agreed with previous studies showing that *Fungi* such as *Pleurotus ostreatus, Coriolopsis polysona,* presented a decreased growth and/or metabolic activity instead of cell death in presence of PCBs [48, 49]. Moreover, the low number of sequences affiliated with *Archaea* agreed with previous studies showing that in soils only 0.5 to 3.8% of the prokaryotes living were *Archaea* [50].

5.2 Taxonomic groups with known mechanisms involved in PCB transformation

First, it is not surprising that microorganisms found in PCB-polluted sample groups with PCB degrading abilities are certainly tolerant to PCBs. In this way, among Bacteria, *Gammaproteobacteria* (*Proteobacteria*), included species known to degrade PCBs and detected in this study as one dominant class under PCB contamination, were previously reported in PCB-contaminated sites with 100 $mg.kg^{-1}$ or over than 700 $mg.kg^{-1}$ dry mass of total PCB [7, 23] suggesting their ubiquity in PCB polluted soils. More specifically, *Gammaproteobacteria* (*Xanthomonadaceae*, *Acidithiobacillaceae* and *Rhodanobacteraceae* families) was abundant under PCB contamination in Pont de Claix and included

363 species known to degrade PCBs thanks to their *bph* genes [51, 52]. Even if *Chloroflexi* bacteria were
364 detected, the *Dehalococcoidia* (*Chloroflexi*) class, known to bear commonly the *rdh* genes [51] involved
365 in PCB transformation under anaerobic condition, was not detected in this study. Interestingly, three
366 other classes of *Chloroflexi* showed lower abundance from P0 to P4 suggesting no PCB tolerance.

367 Concerning *Fungi*, (same trend in 18S rRNA and ITS datasets) species among *Basidiomycota* and
368 *Ascomycota* were known to partially transform PCBs, especially species from the *Saccharomycetes* as
369 previously reported [53], retrieved as well in the present work. Even if the mechanisms involved were
370 not demonstrated for its class, with specifically higher abundance in P2 and P4 groups, *Saccharomycetes*
371 species able to transform PCB in a context of bacteria-yeast consortium are known [53]. The
372 *Pleurotaceae* family (*Basidiomycota*), including the well-known PCB degrader *Pleurotus ostreatus* [7],
373 was specifically retrieved in this study with a higher abundance in the most contaminated groups. For
374 other *Basidiomycota* such as *Pleurotus ostreatus* or *Trametes versicolor*, PCB transformation might be
375 the result of laccases activities whereas, for *Ascomycota* with *Acremonium sclerotigenum*, it would
376 involve peroxidase production [9, 54]. Theses finding suggested that PCB might promote microbial
377 growth. But considering that potential complete PCB transformation might involve diverse
378 microorganisms harboring complex biological pathways and regarding the PCB concentrations still in
379 these soil samples, PCB might rather generate a selection pressure as mentioned above.

380 ### 5.3 Taxonomic groups with potential PCB-transforming mechanisms

381 The *Deltaproteobacteria* and *Gemmatimonadetes* classes could be related to PCB degradation and/or
382 tolerate these molecules because species of these classes were retrieved in PCB polluted soil [51, 52, 55].
383 Moreover, at the family taxonomic level, *Xanthomonadaceae* were known to be able to degrade
384 ethylbenzene and such bacteria might transform or tolerate PCB. Indeed, ethylbenzene are structurally
385 close to PCBs and can present chlorine atoms [56]. The present work also highlighted the presence of

386 the *Holophagae* class (*Acidobacteria*), already reported in a work investigating active bacterial
387 communities in a PCB polluted moorland soil [57]. *Rhodanobacteraceae* family abundant in P4 group
388 could tolerate PCB or be involved in PCB transformation because it includes genus known to use
389 biphenyls as sole carbon source [58].

390 Concerning Fungi, the *Hymenogastraceae* (*Basidiomycota*) family presented higher abundances in
391 groups with intermediate PCB pollution levels and was previously reported as representing 3.3% of
392 fungal sequences from root of *Salix purpurea* in a polluted soil to PCB and hydrocarbons [59], suggesting
393 their adaptability to these molecules. Other family such as *Claroideoglomeraceae* (*Glomeromycota*),
394 abundant in P0 and P3 groups were previously retrieved in extreme petroleum hydrocarbon contaminated
395 site [60].

396 ### 5.4 New taxonomic groups retrieved under PCB contamination

397 To our knowledge, our study reported for the first-time microbial taxa abundant in the soil samples in
398 presence of PCBs, not previously related to these molecules or contaminated ecosystems. In this way
399 these reported microorganisms could be subject of further PCB-transformation assays. The abundance
400 of the *Orbiliomycetes* (*Ascomycota*) class under PCB contamination suggested their tolerance and
401 adaptability to these molecules. It is interesting to note that non-affiliated sequences were few in the low
402 contaminated P0 group of the brownfield compared to the other groups characterized by a higher PCB
403 contamination level. This finding suggested that many microorganisms possibly tolerant and adapted to
404 PCBs are still uncharacterized and knowledge about microbial diversity being present under polluted
405 conditions, like the present work, are necessary to better understand PCB adaptation and further guide
406 bioremediation. To our knowledge, microeucaryotes (other than fungi) were never studied in a PCB
407 contaminated ecosystem. Concerning these under-studied microeucaryotes, *Intramacronucleata*
408 (*Ciliophora*), *Vampyrellidae* (*Cercozoa*), *Arcellinida* and *Euamoebida* (both belonging to *Amoebozoa*)

409 classes and the families such as *Colpodea*, *Nassophorea* (both belonging to *Ciliophora*) showed
410 abundances increased with PCB concentrations suggesting that they might tolerate and be adapt to this
411 molecule directly or by interacting with other adapted fungal or bacterial microorganisms.

412 # 6 Conclusions

413 This work assessed the structure of prokaryotic, micro-eukaryotic and fungal communities for the first
414 time in a PCB gradient from a contaminated brownfield. Because complete PCB transformation might
415 involve several microorganisms not regrouped at the same place in the environment, PCBs are still
416 concentrated in this soil since many years. This *in situ* analysis highlighted that microbial community
417 structure differed depending on PCB concentration. These molecules might act as selection pressure on
418 bacterial and fungal species with some possibly involved in partial PCB transformation. Indeed,
419 microbial structure of low-polluted samples was segregated from polluted samples, especially for the
420 prokaryotic communities. Interestingly, the microbial abundance tended to be more important with
421 increasing PCB concentrations. These results showed that PCBs seems to act as a selection pressure.
422 These molecules impacted the three-domain of microbial life composition and could select adapted
423 microorganisms, possibly able to transform PCBs, developing favorable coexistence. However, all these
424 results need to be confirmed by further analyses involving greater number of samples and *in vitro*
425 biotransformation demonstration. Other taxa listed here were also retrieved for the first time in polluted
426 samples but their potential PCB tolerance and/or biotransformation remained unknown and might be
427 promising. That is why further ecotoxicological studies will allow gaining into exhaustive microbial
428 diversity presenting in PCB polluted ecosystems to support and guide future PCB bioremediation studies.

7 Statements & Declarations

This work was supported by the French MITI-CNRS [urban ecosystem - AAP 2019], EC2CO – CNRS [CNRS INSU - AAP 2020] and French Auvergne-Rhône-Alpes AURA Region [Pack Ambition Recherche 2021] programs. F. Maucourt PhD was supported by a Research and Technology French National association ANRT and Envisol fellowship. The authors have no relevant financial or non-financial interests to disclose. All authors contributed to the study conception and design. Material preparation and data collection were performed by F. Maucourt, A. Cébron, H. Budzinski, K. Le Ménach, L. Peluhet, D. Chapulliot, L. Vallon, S. Czarnes and M. Hugoni. Data analyses were performed by F. Maucourt, A. Cébron, M. Hugoni and L. Fraissinet-Tachet. The first draft of the manuscript was written by F. Maucourt and all authors commented on previous versions of the manuscript. All authors read and approved the final manuscript. We would like to thank Jean Thioulouse (LBBE - UMR CNRS 5558 - Villeurbanne) for helpful discussions.

8 Data availability

All data that support findings of this study have been deposited in European Nucleotide Archive (https://www.ebi.ac.uk/ena/browser/view/PRJEB46614) under reference PRJEB46614 for 16S rRNA dataset, PRJEB46555 and PRJEB46556 for ITS regions and eukaryotic 18S rRNA genes, respectively.

9 References

1. Wall DH, Behan-Pelletier V, Jones TH, et al (2012) Soil Ecology and Ecosystem Services. OUP Oxford
2. Beaudette LA, Davies S, Fedorak PM, et al (1998) Comparison of Gas Chromatography and Mineralization Experiments for Measuring Loss of Selected Polychlorinated Biphenyl Congeners in Cultures of White Rot Fungi. Appl Env Microbiol 64:2020–2025
3. Weltgesundheitsorganisation, International Programme on Chemical Safety, Inter-Organization Programme for the Sound Management of Chemicals (2003) Polychlorinated biphenyls: human health aspects. World Health Organization, Geneva

4. Pointing S (2001) Feasibility of bioremediation by white-rot fungi. Appl Microbiol Biotechnol 57:20–33. https://doi.org/10.1007/s002530100745
5. Arbon RE, Mincher BJ, Knighton WB (1994) .gamma.-Ray Destruction of Individual PCB Congeners in Neutral 2-propanol. Environ Sci Technol 28:2191–2196. https://doi.org/10.1021/es00061a030
6. Pieper DH, Seeger M (2008) Bacterial Metabolism of Polychlorinated Biphenyls. J Mol Microbiol Biotechnol 15:121–138. https://doi.org/10.1159/000121325
7. Stella T, Covino S, Čvančarová M, et al (2017) Bioremediation of long-term PCB-contaminated soil by white-rot fungi. J Hazard Mater 324:701–710. https://doi.org/10.1016/j.jhazmat.2016.11.044
8. Tigini V, Prigione V, Di Toro S, et al (2009) Isolation and characterisation of polychlorinated biphenyl (PCB) degrading fungi from a historically contaminated soil. Microb Cell Factories 8:5–19. https://doi.org/10.1186/1475-2859-8-5
9. Germain J, Raveton M, Binet MN, Mouhamadou B (2021) Screening and metabolic potential of fungal strains isolated from contaminated soil and sediment in the polychlorinated biphenyl degradation. Ecotoxicol Environ Saf 208:111703. https://doi.org/10.1016/j.ecoenv.2020.111703
10. Hashmi MZ, Qin Z, Yao X, et al (2016) PCBs attenuation and abundance of Dehalococcoides spp., bphC, CheA, and flic genes in typical polychlorinated biphenyl-polluted soil under floody and dry soil conditions. Environ Sci Pollut Res 23:3907–3913. https://doi.org/10.1007/s11356-015-5577-1
11. Sharma JK, Gautam RK, Nanekar SV, et al (2018) Advances and perspective in bioremediation of polychlorinated biphenyls contaminated soils. Environ Sci Pollut Res Int 25:16355–16375. https://doi.org/10.1007/s11356-017-8995-4
12. Pino NJ, Múnera LM, Peñuela GA (2019) Phytoremediation of soil contaminated with PCBs using different plants and their associated microbial communities. Int J Phytoremediation 21:316–324. https://doi.org/10.1080/15226514.2018.1524832
13. Steliga T, Wojtowicz K, Kapusta P, Brzeszcz J (2020) Assessment of Biodegradation Efficiency of Polychlorinated Biphenyls (PCBs) and Petroleum Hydrocarbons (TPH) in Soil Using Three Individual Bacterial Strains and Their Mixed Culture. Molecules 25:709. https://doi.org/10.3390/molecules25030709
14. Borja J, Taleon DM, Auresenia J, Gallardo S (2005) Polychlorinated biphenyls and their biodegradation. Process Biochem 40:1999–2013. https://doi.org/10.1016/j.procbio.2004.08.006
15. Furukawa K, Fujihara H (2008) Microbial degradation of polychlorinated biphenyls: Biochemical and molecular features. J Biosci Bioeng 105:433–449. https://doi.org/10.1263/jbb.105.433
16. Sietmann R, Gesell M, Hammer E, Schauer F (2006) Oxidative ring cleavage of low chlorinated biphenyl derivatives by fungi leads to the formation of chlorinated lactone derivatives. Chemosphere 64:672–685. https://doi.org/10.1016/j.chemosphere.2005.10.050
17. Kohlmeier S, Smits THM, Ford RM, et al (2005) Taking the Fungal Highway: Mobilization of Pollutant-Degrading Bacteria by Fungi. Environ Sci Technol 39:4640–4646. https://doi.org/10.1021/es047979z
18. Wei Y, Wang X, Liu J, et al (2011) The population dynamics of bacteria in physically structured habitats and the adaptive virtue of random motility. Proc Natl Acad Sci 108:4047–4052. https://doi.org/10.1073/pnas.1013499108
19. Čvančarová M, Křesinová Z, Filipová A, et al (2012) Biodegradation of PCBs by ligninolytic fungi and characterization of the degradation products. Chemosphere 88:1317–1323. https://doi.org/10.1016/j.chemosphere.2012.03.107

20. Mouhamadou B, Faure M, Sage L, et al (2013) Potential of autochthonous fungal strains isolated from contaminated soils for degradation of polychlorinated biphenyls. Fungal Biol 117:268–274. https://doi.org/10.1016/j.funbio.2013.02.004
21. Sage L, Périgon S, Faure M, et al (2014) Autochthonous ascomycetes in depollution of polychlorinated biphenyls contaminated soil and sediment. Chemosphere 110:62–69. https://doi.org/10.1016/j.chemosphere.2014.03.013
22. Nogales B, Moore ERB, Llobet-Brossa E, et al (2001) Combined Use of 16S Ribosomal DNA and 16S rRNA To Study the Bacterial Community of Polychlorinated Biphenyl-Polluted Soil. Appl Environ Microbiol 67:1874–1884. https://doi.org/10.1128/AEM.67.4.1874-1884.2001
23. Zenteno-Rojas A, Martínez-Romero E, Castañeda-Valbuena D, et al (2020) Structure and diversity of native bacterial communities in soils contaminated with polychlorinated biphenyls. AMB Express 10:124. https://doi.org/10.1186/s13568-020-01058-8
24. Ding N, Hayat T, Wang J, et al (2011) Responses of microbial community in rhizosphere soils when ryegrass was subjected to stress from PCBs. J Soils Sediments 11:1355–1362. https://doi.org/10.1007/s11368-011-0412-x
25. Marchal C, Germain J, Raveton M, et al (2021) Molecular Characterization of Fungal Biodiversity in Long-Term Polychlorinated Biphenyl-Contaminated Soils. Microorganisms 9:2051. https://doi.org/10.3390/microorganisms9102051
26. Cébron A, Beguiristain T, Bongoua-Devisme J, et al (2015) Impact of clay mineral, wood sawdust or root organic matter on the bacterial and fungal community structures in two aged PAH-contaminated soils. Environ Sci Pollut Res 22:13724–13738. https://doi.org/10.1007/s11356-015-4117-3
27. Schnürer J, Rosswall T (1982) Fluorescein Diacetate Hydrolysis as a Measure of Total Microbial Activity in Soil and Litter. Appl Environ Microbiol 43:1256–1261. https://doi.org/10.1128/aem.43.6.1256-1261.1982
28. Caporaso JG, Lauber CL, Walters WA, et al (2011) Global patterns of 16S rRNA diversity at a depth of millions of sequences per sample. Proc Natl Acad Sci 108:4516–4522. https://doi.org/10.1073/pnas.1000080107
29. Wang Y, Qian P-Y (2009) Conservative Fragments in Bacterial 16S rRNA Genes and Primer Design for 16S Ribosomal DNA Amplicons in Metagenomic Studies. PLOS ONE 4:e7401. https://doi.org/10.1371/journal.pone.0007401
30. Russo DA, Couto N, Beckerman AP, Pandhal J (2016) A Metaproteomic Analysis of the Response of a Freshwater Microbial Community under Nutrient Enrichment. Front Microbiol 7:1172. https://doi.org/10.3389/fmicb.2016.01172
31. Hugoni M, Escalas A, Bernard C, et al (2018) Spatiotemporal variations in microbial diversity across the three domains of life in a tropical thalassohaline lake (Dziani Dzaha, Mayotte Island). Mol Ecol 27:4775–4786. https://doi.org/10.1111/mec.14901
32. Rognes T, Flouri T, Nichols B, et al (2016) VSEARCH: a versatile open source tool for metagenomics. PeerJ 4:e2584. https://doi.org/10.7717/peerj.2584
33. Mahé F, Rognes T, Quince C, et al (2014) Swarm: robust and fast clustering method for amplicon-based studies. PeerJ 2:e593
34. Bokulich NA, Subramanian S, Faith JJ, et al (2013) Quality-filtering vastly improves diversity estimates from Illumina amplicon sequencing. Nat Methods 10:57–59. https://doi.org/10.1038/nmeth.2276

35. Wang Q, Garrity GM, Tiedje JM, Cole JR (2007) Naive Bayesian classifier for rapid assignment of rRNA sequences into the new bacterial taxonomy. Appl Environ Microbiol 73:5261–5267. https://doi.org/10.1128/AEM.00062-07
36. Camacho C, Coulouris G, Avagyan V, et al (2009) BLAST+: architecture and applications. BMC Bioinformatics 10:421. https://doi.org/10.1186/1471-2105-10-421
37. Glöckner FO, Yilmaz P, Quast C, et al (2017) 25 years of serving the community with ribosomal RNA gene reference databases and tools. J Biotechnol 261:169–176. https://doi.org/10.1016/j.jbiotec.2017.06.1198
38. Escudié F, Auer L, Bernard M, et al (2017) FROGS: Find, Rapidly, OTUs with Galaxy Solution. Bioinformatics. https://doi.org/10.1093/bioinformatics/btx791
39. Gower JC (1971) A General Coefficient of Similarity and Some of Its Properties. Biometrics, pp 857–871
40. Dixon P (2003) VEGAN, a package of R functions for community ecology. J Veg Sci 14:927–930. https://doi.org/10.1111/j.1654-1103.2003.tb02228.x
41. R Development Core Team (2010) a language and environment for statistical computing: reference index. R Foundation for Statistical Computing, Vienna
42. Wickham H (2010) A Layered Grammar of Graphics. J Comput Graph Stat 19:3–28. https://doi.org/10.1198/jcgs.2009.07098
43. Hammer O, Harper DAT, Ryan PD (2001) PAST: Paleontological Statistics Software Package for Education and Data Analysis. Palaeontol Electron 4:9
44. Ramette A (2007) Multivariate analyses in microbial ecology. FEMS Microbiol Ecol 62:142–160. https://doi.org/10.1111/j.1574-6941.2007.00375.x
45. Mackova M, Prouzova P, Stursa P, et al (2009) Phyto/rhizoremediation studies using long-term PCB-contaminated soil. Environ Sci Pollut Res 16:817–829. https://doi.org/10.1007/s11356-009-0240-3
46. Hu J, Qian M, Zhang Q, et al (2015) Sphingobium fuliginis HC3: A Novel and Robust Isolated Biphenyl- and Polychlorinated Biphenyls-Degrading Bacterium without Dead-End Intermediates Accumulation. PLOS ONE 10:e0122740. https://doi.org/10.1371/journal.pone.0122740
47. Muzikář M, Křesinová Z, Svobodová K, et al (2011) Biodegradation of chlorobenzoic acids by ligninolytic fungi. J Hazard Mater 196:386–394. https://doi.org/10.1016/j.jhazmat.2011.09.041
48. Ruiz-aguilar GML, Fern JM, Rodrıguez-vazquez R, Poggi-varaldo H (2001) Degradation by white-rot fungi of high concentrations of PCB
49. Vyas BRM, Šašek V, Matucha M, Bubner M (1994) Degradation of 3,3′,4,4′-tetrachlorobiphenyl by selected white rot fungi. Chemosphere 28:1127–1134. https://doi.org/10.1016/0045-6535(94)90331-X
50. Timonen S, Bomberg M (2009) Archaea in dry soil environments. Phytochem Rev 8:505–518. https://doi.org/10.1007/s11101-009-9137-5
51. Khalid F, Hashmi MZ, Jamil N, et al (2021) Microbial and enzymatic degradation of PCBs from e-waste-contaminated sites: a review. Environ Sci Pollut Res 28:. https://doi.org/10.1007/s11356-020-11996-2
52. Matturro B, Mascolo G, Rossetti S (2020) Microbiome changes and oxidative capability of an anaerobic PCB dechlorinating enrichment culture after oxygen exposure. New Biotechnol 56:96–102. https://doi.org/10.1016/j.nbt.2019.12.004
53. Romero MC, Reinoso EH, Moreno Kiernan A, Urrutia MI (2006) Chlorinated biphenyl degradation by wild yeasts pre-cultured in biphasic systems. Electron J Biotechnol 9:0–0. https://doi.org/10.4067/S0717-34582006000300013

54. Périgon S, Massier M, Germain J, et al (2019) Metabolic adaptation of fungal strains in response to contamination by polychlorinated biphenyls. Environ Sci Pollut Res 26:14943–14950. https://doi.org/10.1007/s11356-019-04701-5
55. Cervantes-González E, Guevara-García MA, García-Mena J, Ovando-Medina VM (2019) Microbial diversity assessment of polychlorinated biphenyl–contaminated soils and the biostimulation and bioaugmentation processes. Environ Monit Assess 191:118. https://doi.org/10.1007/s10661-019-7227-4
56. Jayamani I, Cupples AM (2015) Stable Isotope Probing and High-Throughput Sequencing Implicate *Xanthomonadaceae* and *Rhodocyclaceae* in Ethylbenzene Degradation. Environ Eng Sci 32:240–249. https://doi.org/10.1089/ees.2014.0456
57. Nogales B, Moore ERB, Abraham W-R, Timmis KN (1999) Identification of the metabolically active members of a bacterial community in a polychlorinated biphenyl-polluted moorland soil. Environ Microbiol 1:199–212. https://doi.org/10.1046/j.1462-2920.1999.00024.x
58. McGenity TJ (2019) Taxonomy, Genomics and Ecophysiology of Hydrocarbon-Degrading Microbes. Springer International Publishing, Cham
59. Gonzalez E, Pitre FE, Pagé AP, et al (2018) Trees, fungi and bacteria: tripartite metatranscriptomics of a root microbiome responding to soil contamination. Microbiome 6:53. https://doi.org/10.1186/s40168-018-0432-5
60. Kong M, St-Arnaud M, Hijri M, Laliberté É (2016) Biodiversity of Arbuscular Mycorrhizal Fungi from Extreme Petroleum Hydrocarbon Contaminated Site. 65
61. Budzinski JW, Foster BC, Vandenhoek S, Arnason JT (2000) An in vitro evaluation of human cytochrome P450 3A4 inhibition by selected commercial herbal extracts and tinctures. Phytomedicine 7:273–282. https://doi.org/10.1016/S0944-7113(00)80044-6
62. Barhoumi B, LeMenach K, Dévier M-H, et al (2014) Distribution and ecological risk of polychlorinated biphenyls (PCBs) and organochlorine pesticides (OCPs) in surface sediments from the Bizerte lagoon, Tunisia. Environ Sci Pollut Res 21:6290–6302. https://doi.org/10.1007/s11356-013-1709-7

Table and Figures

Table 1. Indicator PCB pollution concentration by sample

	Zone 2 (Z2)										Zone 3/4 (Z3/4)									
	F1	**F2**	**F3**	**F4**	**F5**	**B1**	**B2**	**B3**	**B4**	**B5**	**B1**	**B2**	**B3**	**B4**	**B5**	**E1**	**E2**	**E3**	**E4**	**E5**
PCB 28	1.02	0.27	0.56	4.9	<0.01	2.29	0.12	0.03	0.07	0.03	0.04	0.17	0.24	0.74	<0.01	0.67	0.35	0.33	0.91	0.22
PCB 52	5.5	1.2	2.24	11.4	0.05	6.22	0.56	0.05	0.28	0.16	0.28	0.63	0.89	1.7	0.02	2.08	1.46	1.65	2.04	1.37
PCB 101	2.76	0.59	1.05	5.59	0.03	4.72	0.25	0.02	0.18	0.11	0.23	0.48	0.38	1	0.01	1.76	0.84	1.44	1.01	0.71
PCB 118	2.11	0.47	0.86	4.48	0.03	4.64	0.19	0.01	0.14	0.09	0.16	0.65	0.31	0.89	<0.01	1.27	0.51	0.84	0.87	0.51
PCB 138	1.11	0.33	0.43	2.05	0.03	1.45	0.28	0.02	0.08	0.05	0.4	0.5	0.19	0.41	<0.01	1.74	0.63	1.21	1.18	0.43
PCB 153	1.01	0.29	0.35	1.97	0.02	1.75	0.23	0.02	0.07	0.05	0.3	0.58	0.16	0.34	<0.01	1.87	0.53	1.49	0.95	0.37
PCB 180	0.46	0.14	0.18	0.72	0.01	0.56	0.13	0.01	0.02	0.02	0.26	0.24	0.05	0.25	<0.01	1.18	0.34	0.6	0.73	0.22
Total	14	3.29	5.67	31.1	0.17	21.6	1.76	0.16	0.84	0.51	1.67	3.25	2.22	5.33	0.03	10.6	4.66	7.56	7.69	3.83

Figure 1. Hierarchical clustering of samples and microbial community structure by NMDS

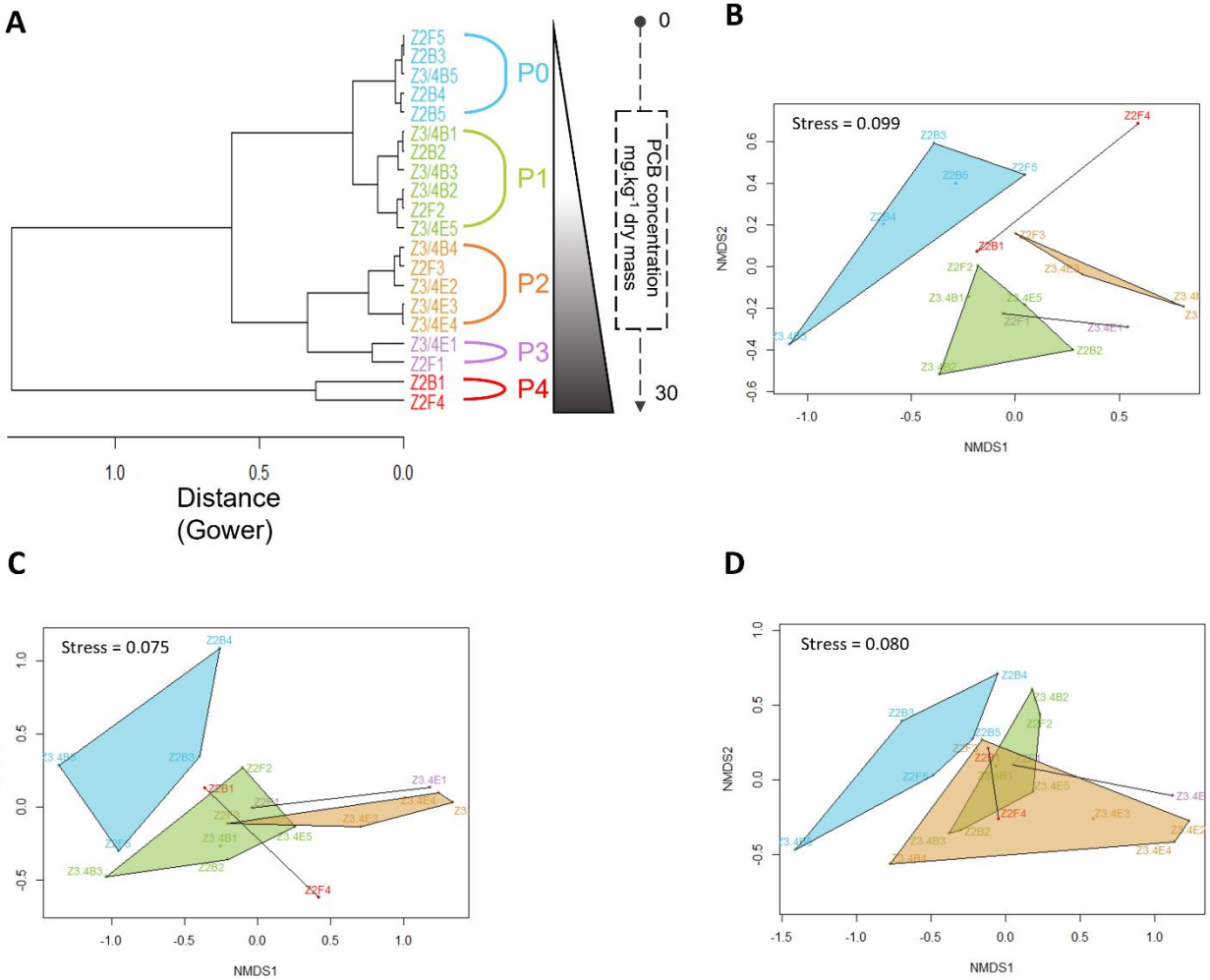

Figure 2. The bacterial taxonomic composition

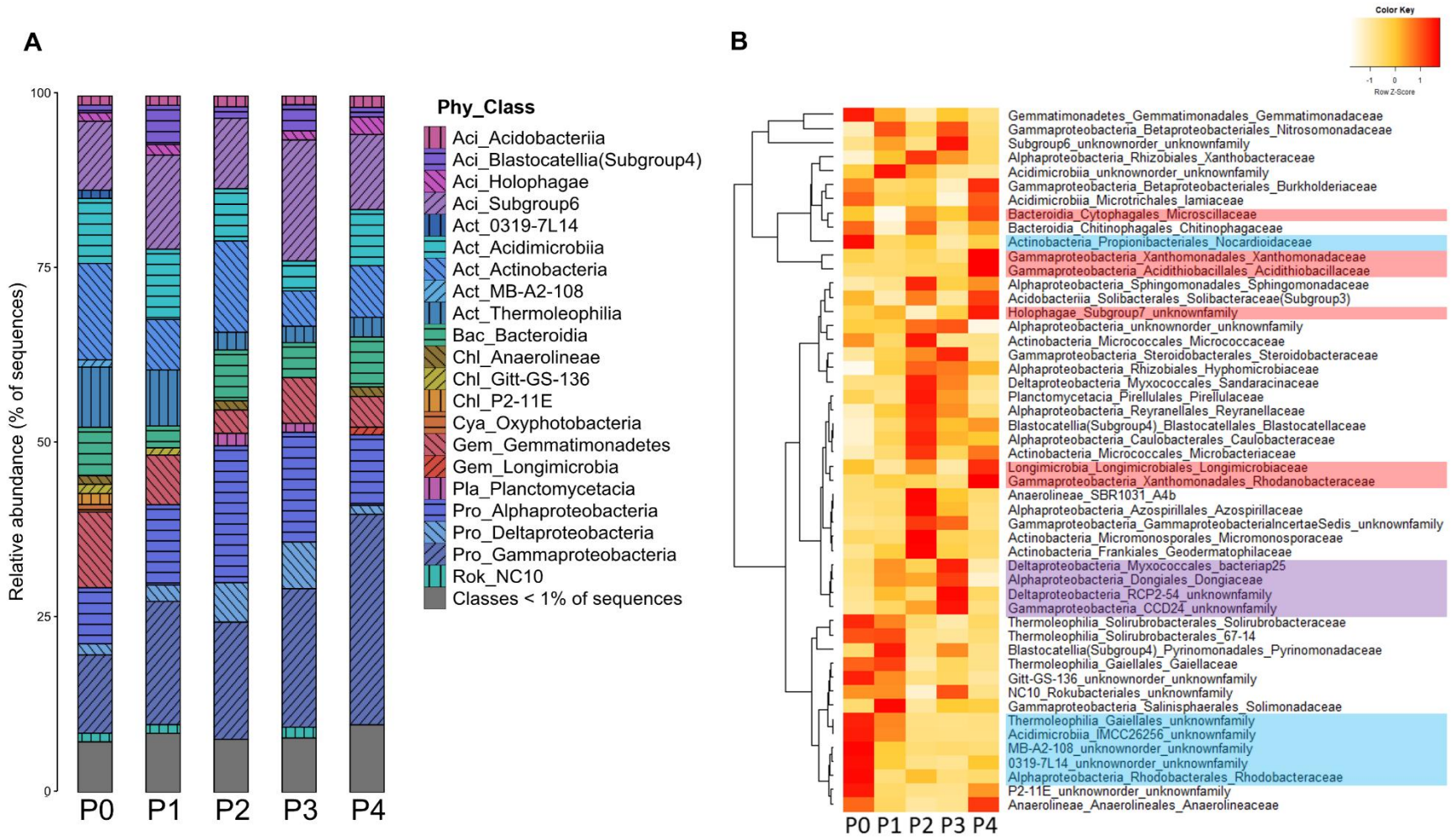

626 **Figure 3. The eukaryotic taxonomic composition**

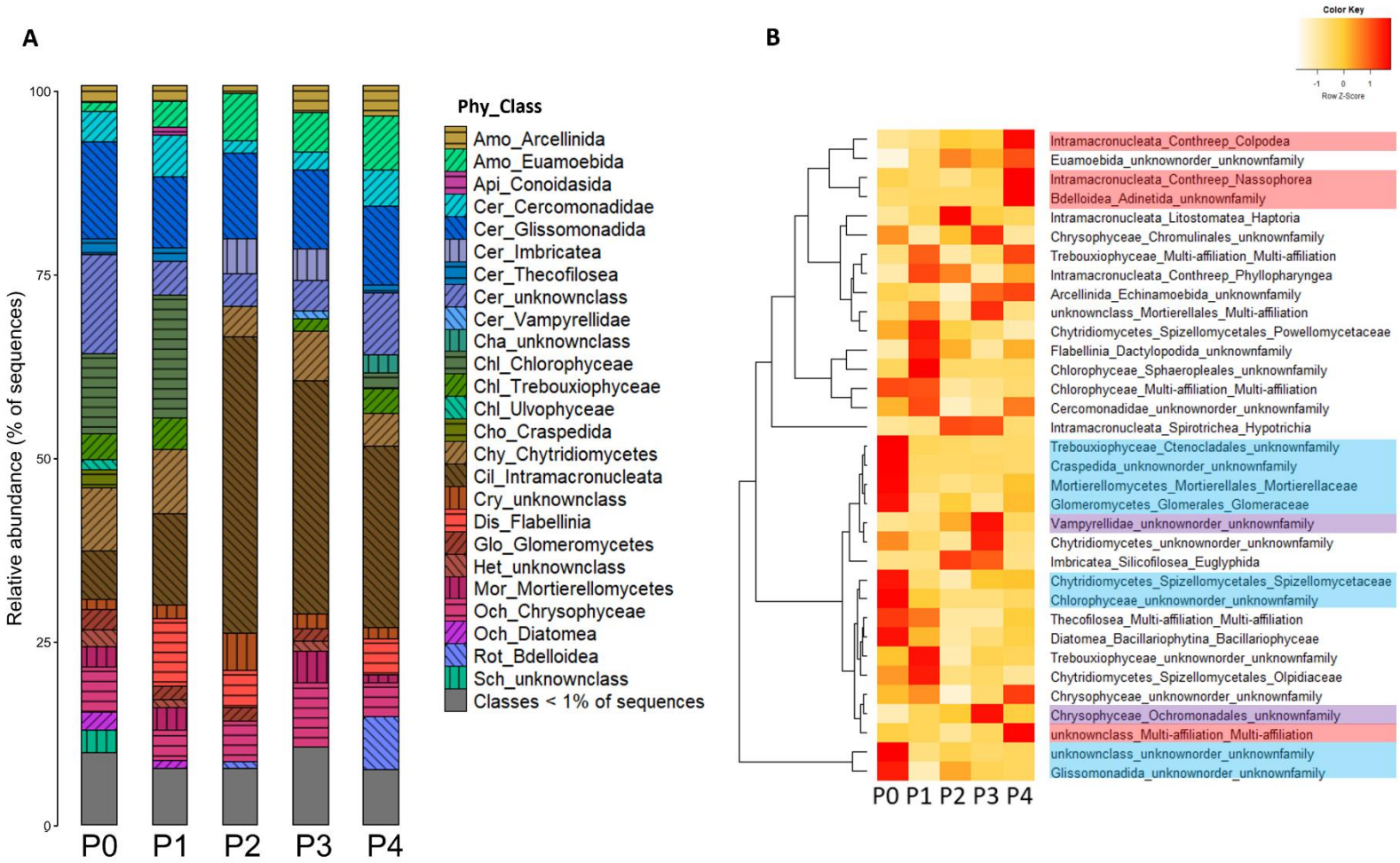

627

Figure 4. The fungal taxonomic composition

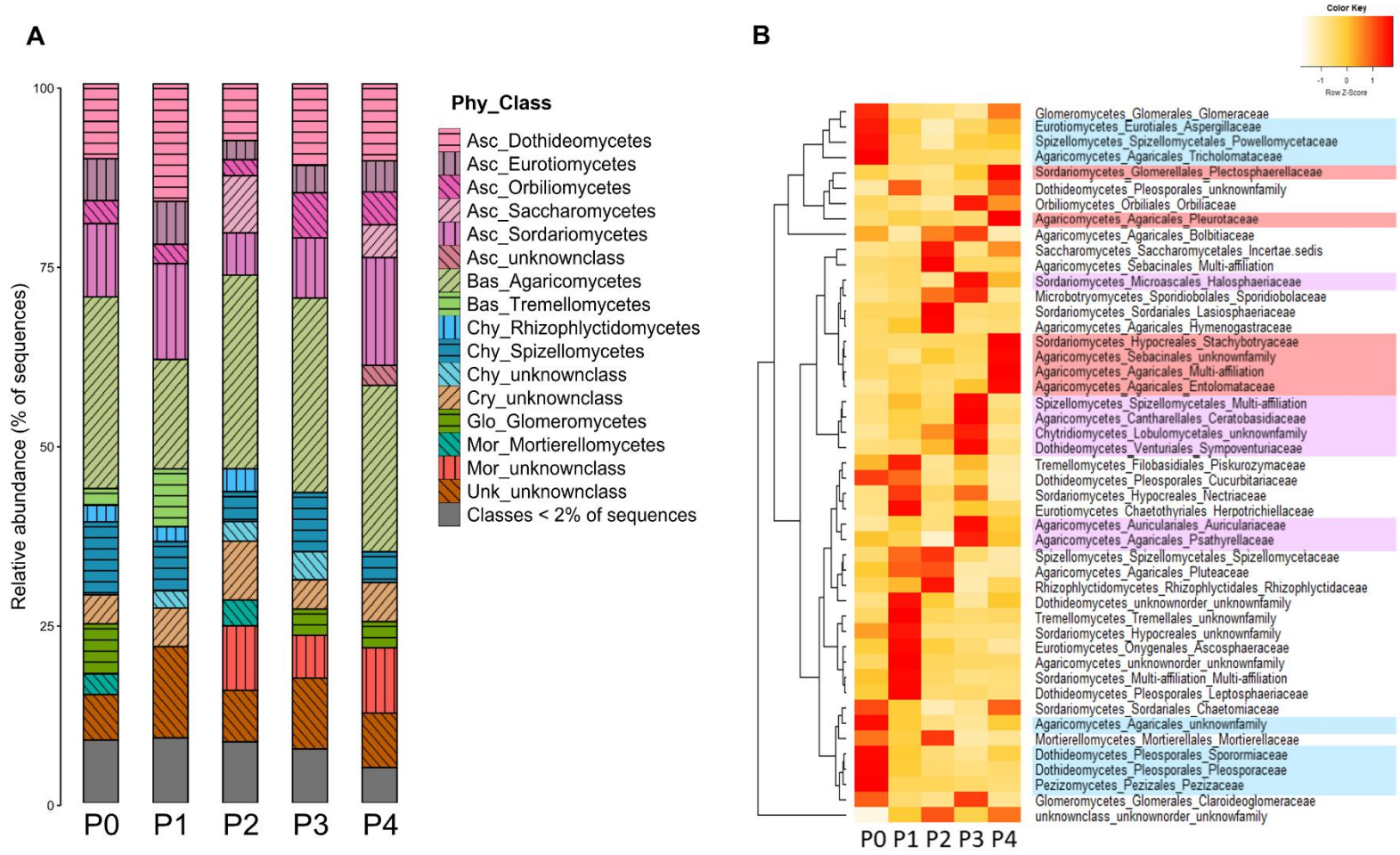

Supplementary Experimental Procedures

9.1 Soil physico-chemical analyses

Physico-chemical properties of the soil were evaluated at the CESAR laboratory (http://www.labo-cesar.com/, Ceyzeriat, France) by analyzing the soil samples Z2B5, Z2F2, Z2F3, Z2F1 and Z2F4, representing the P0, P1, P2, P3 and P4 groups respectively. The cation exchange capacity (CEC), soil pH (H_20), pH (KCl) and soil texture were assessed according to technical standard procedures, together with the contents of total organic carbon and total nitrogen.

9.2 C-CO_2 Microbial mineralization and enzymatic biological activity assay

Three replicates per soil sample were monitored for microbial mineralization, and empty control flasks without soil were run in the same way to correct for basal atmospheric CO_2 measurement. The produced CO_2 of each sample was expressed as carbon mass per gram of dry weight soil. After each measurement, flasks were opened for 15 min under a fume hood for aeration to avoid anoxia through accumulation of CO_2, and humidity was adjusted with sterile water. Flasks were sealed and incubated again. Measurements were performed after 3, 7, 11, 14 and 19 days of incubation. The microbial activity was evaluated on soil samples Z2B5, Z2F2, Z2F3, Z2F1 and Z2F4 (representing P0, P1, P2, P3 and P4 groups respectively). This FDA hydrolase enzymatic test is non-specific and integrates the activity of many fungal and bacterial enzymes such as esterases, lipases, proteases secreted in soils by microorganisms.

9.3 Additional PCB assay analyses

Chemical analyses were performed on the soil samples, after freeze-drying and sieving at 2 mm. Chemical analyses focused on 71 congeners of polychlorinated biphenyls (PCBs). PCB analyses were performed as described previously [61]. Soil samples were extracted using

654 micro-wave assisted extraction [61]and extract clean-up was carried out on a multilayer column
655 (alumina and silica with activated copper). Extracts were purified on acid-impregnated silica
656 and quantified by gas chromatography coupled with electron capture detection (GC-ECD) [62]
657 using internal standard quantification with PCBs not present in environment (PCBs 30, 103,
658 155, 198) and 4,4'-DDT-d8 as internal standards. Procedural blanks were performed for each
659 sample batch and blank-correction was applied. Samples and blanks were spiked with internal
660 recovery standards prior to extraction procedures and with a syringe standard (octachloro-
661 naphthalene) before injection to monitor IS losses; recoveries higher than 60% were accepted.
662 Limits of detection (LODs) and limits of quantification (LOQs) were set as the concentrations
663 yielding signal-to-noise ratios of 3 and 10, respectively. LOQs were in the range 0.03–5 ng g^{-1}
664 dw of PCBs.

Supplementary results

9.1 Core *versus* specific microbiome among PCB pollution

For the prokaryotic dataset (Figure S3), OTUs from three families were specific to P0, consisting in *Entotheonellaceae (Tectomicrobia),* and the uncharacterized *Blfdi19* and *P3OB-42* (both from *Proteobacteria*). The *Segniliparaceae* family (*Actinobacteria)* was specific to P1 group. Both families *Sandaracinaceae* (*Proteobacteria*) and the uncharacterized *A4b* one *(Chloroflexi)* were specific to the P2 group. The *Dysgonomonadaceae (Bacteroidetes), Parvibaculaceae* and the uncharacterized *A0839* (both from *Proteobacteria*) families were specific to the P4 group.

For microeukaryotic communities (Figure S4), OTUs from the *Labyrinthulomyceae (Stramenopiles)* and the *Mortierellaceae* (*Mortierellomycota*) families were specific to the P0 group. OTUs specific of the P1 group were belonging to families from *Armophorida* order, *Eimeriorina* suborder (both belonging to *Alveolata)* and to the *Rhizaspididae* family (from *Rhizaria*).

Concerning fungal OTUs families (Figure S5), *Ascophaeraceae (Eurotiomycetes), Basidiobollaceae (Basidiobolomycetes), Glomeraceae (Glomeromycetes), Gymnoascaceae (Eurotiomycetes), Protrudomycetaceae (Rhizophyudiomycetes), Crepidotaceae, Hymenogastraceae* and *Tricholomataceae (these three last families belonging to Agaricomycetes)* were the specific P0 families. *Ascobolacea (Pezizomycetes), Helotiaceae (Leotiomycetes), Metschnikowiaceae (Saccharomycetes), Sporidiobolaceae (Microbotryomycetes), Leptosphaeriaceae* and *Sporormiaceae* (both belonging to *Dothideomycetes*), *Ustilaginaceae (Ustilaginomycetes), Vuilleminiaceae (Agaricomycetes), Magnaporthaceae, Microdochiaceae* and *Xylariaceae* (these three last families belonging to *Sordariomycetes)* were specific to P1 group. *Pezizaceae (Pezizomycetes), Sebacinaceae* and *Sereundipitaceae* (both belonging to *Agaromycetes)* were families specific to P2 group.

690 *Pluteaceae* and *Psathyrellaceae* (both from *Agaricomycetes*) were families specific to P3
691 group.

Supplementary tables and figures

Table S1. Physicochemical characteristics of the soil sampling site

	Clay ($g.kg^{-1}$)	Silt ($g.kg^{-1}$)	Sand ($g.kg^{-1}$)	Total Organic Carbon ($g.kg^{-1}$)	Total Nitrogen ($g.kg^{-1}$)	C/N	CEC ($cmol.kg^{-1}$)	pH (Water)	pH (KCl)
P0	143	675	182	8.16	1.04	8	4.933	8.42	7.84
P1	99	222	679	7.98	1.03	8	3.043	8.59	7.97
P3	50	109	842	9.26	0.68	14	1.921	8.74	8.22
P3	96	256	648	4.83	0.59	8	2.428	8.56	7.95
P4	114	464	422	30.16	1.06	28	3.54	8.37	7.59

Table S2. Concentration of 71 different PCB by sample

	Zone 2 (Z2)										Zone 3/4 (Z3/4)									
	F1	**F2**	**F3**	**F4**	**F5**	**B1**	**B2**	**B3**	**B4**	**B5**	**B1**	**B2**	**B3**	**B4**	**B5**	**E1**	**E2**	**E3**	**E4**	**E5**
CB 1	0.0	0.0	0.0	0.0	0.0	0.0	0.0	0.0	0.0	0.0	0.0	0.0	0.0	0.0	0.0	0.0	0.0	0.0	0.0	0.0
CB 3	0.0	0.0	0.0	0.0	0.0	0.0	0.0	0.0	0.0	0.0	0.0	0.0	0.0	0.0	0.0	0.0	0.0	0.0	0.0	0.0
CB 10/4	0.0	0.0	0.0	0.0	0.0	0.0	0.0	0.0	0.0	0.0	0.0	0.0	0.0	0.0	0.0	0.0	0.0	0.0	0.0	0.0
CB 8	0.0	0.0	0.0	0.0	0.0	0.0	0.0	0.0	0.0	0.0	0.0	0.0	0.0	0.0	0.0	0.0	0.0	0.0	0.0	0.0
CB 19	0.0	0.0	0.0	1.3	0.0	0.1	0.0	0.0	0.0	0.0	0.0	0.0	0.0	0.0	0.0	0.0	0.0	0.0	0.0	0.0
CB 18	0.2	0.1	0.2	2.8	0.0	0.3	0.1	0.0	0.0	0.0	0.0	0.1	0.0	0.1	0.0	0.2	0.2	0.1	0.3	0.1
CB 15	0.2	0.1	0.2	2.6	0.0	0.9	0.1	0.0	0.0	0.0	0.0	0.0	0.1	0.1	0.0	0.2	0.2	0.1	0.2	0.1
CB 29/54	0.0	0.0	0.0	0.0	0.0	0.0	0.0	0.0	0.0	0.0	0.0	0.0	0.0	0.0	0.0	0.0	0.0	0.0	0.0	0.0
CB 50	0.0	0.0	0.0	0.0	0.0	0.0	0.0	0.0	0.0	0.0	0.0	0.0	0.0	0.0	0.0	0.0	0.0	0.0	0.0	0.0
CB 31	0.8	0.3	0.5	5.8	0.0	0.7	0.1	0.0	0.1	0.0	0.0	0.1	0.2	0.4	0.0	0.4	0.4	0.3	0.6	0.2
CB 28	0.8	0.3	0.5	3.8	0.0	1.9	0.1	0.0	0.1	0.0	0.0	0.1	0.2	0.4	0.0	0.5	0.4	0.3	0.4	0.2
CB 33	0.0	0.0	0.1	1.1	0.0	0.1	0.0	0.0	0.0	0.0	0.0	0.0	0.0	0.0	0.0	0.1	0.1	0.0	0.1	0.0

CB 22	1.0	0.0	0.1	1.3	0.0	0.2	0.0	0.0	0.0	0.0	0.0	0.0	0.1	0.1	0.0	0.1	0.1	0.1	0.1	0.0
CB 52	5.0	1.1	2.3	12.0	0.0	6.2	0.4	0.0	0.3	0.1	0.2	0.6	0.7	1.5	0.0	2.0	1.4	1.5	1.4	1.0
CB 49	2.8	0.6	1.3	7.2	0.0	4.8	0.2	0.0	0.2	0.1	0.1	0.3	0.4	0.9	0.0	1.2	0.8	0.8	0.7	0.6
CB 104	0.0	0.0	0.0	0.0	0.0	0.0	0.0	0.0	0.0	0.0	0.0	0.0	0.0	0.0	0.0	0.0	0.0	0.0	0.0	0.0
CB 44	4.0	0.9	2.0	10.2	0.0	6.0	0.4	0.0	0.2	0.1	0.2	0.4	0.6	1.2	0.0	1.6	1.2	1.1	1.1	0.8
CB 41	3.5	0.7	1.8	8.8	0.0	5.7	0.3	0.0	0.2	0.1	0.1	0.3	0.5	0.9	0.0	1.3	0.9	0.9	1.0	0.7
CB 40	0.7	1.5	0.4	1.9	0.0	1.2	0.1	0.0	0.0	0.0	0.0	0.1	0.1	0.2	0.0	0.3	0.2	0.2	0.2	0.1
CB 74	1.7	0.5	0.8	5.4	0.0	4.2	0.1	0.0	0.1	0.0	0.1	0.3	0.3	0.6	0.0	0.6	0.5	0.5	0.7	0.3
CB 70	4.7	1.1	2.1	12.5	0.1	5.3	0.4	0.0	0.3	0.1	0.1	0.6	0.6	1.5	0.0	1.9	1.4	1.3	1.4	0.9
CB 66	5.5	1.3	2.4	12.6	0.1	10.3	0.5	0.0	0.3	0.2	0.2	0.8	0.8	1.7	0.0	2.2	1.6	1.5	1.5	1.1
CB 95	1.6	0.4	0.7	3.8	0.0	2.1	0.2	0.0	0.1	0.1	0.2	0.3	0.3	0.5	0.0	0.9	0.6	0.9	0.6	0.4
CB 60	1.9	0.4	0.9	6.0	0.0	2.7	0.2	0.0	0.1	0.0	0.1	0.3	0.4	0.7	0.0	0.7	0.6	0.5	0.7	0.3
CB 101 + CB90	2.4	0.6	1.0	5.4	0.0	3.1	0.2	0.0	0.2	0.1	0.2	0.5	0.4	0.7	0.0	1.2	0.8	1.1	0.9	0.6
CB 99	1.4	0.3	0.6	3.0	0.0	2.0	0.1	0.0	0.1	0.0	0.1	0.3	0.2	0.4	0.0	0.6	0.4	0.4	0.4	0.3

CB 119	0.8	0.0	0.0	0.1	0.0	0.1	0.0	0.0	0.0	0.0	0.0	0.0	0.0	0.0	0.0	0.0	0.0	0.0	0.0	0.0
CB 81 + CB87	1.7	0.4	0.7	4.1	0.0	1.9	0.2	0.0	0.1	0.0	0.2	0.3	0.3	0.5	0.0	0.7	0.5	0.6	0.5	0.4
CB 77 + CB110	4.1	0.9	1.7	8.9	0.0	5.7	0.4	0.0	0.2	0.1	0.5	0.8	0.6	1.2	0.0	1.8	1.2	1.5	1.2	0.9
CB 154	0.0	0.0	0.0	0.0	0.0	0.0	0.0	0.0	0.0	0.0	0.0	0.0	0.0	0.0	0.0	0.0	0.0	0.0	0.0	0.0
CB 151	0.2	0.1	0.1	0.4	0.0	0.3	0.1	0.0	0.0	0.0	0.1	0.1	0.0	0.1	0.0	0.3	0.1	0.3	0.2	0.1
CB 123/149	0.6	0.2	0.2	1.3	0.0	0.7	0.1	0.0	0.0	0.0	0.2	0.2	0.1	0.2	0.0	0.7	0.4	0.8	0.5	0.2
CB 118	1.8	0.4	0.8	3.9	0.0	2.8	0.2	0.0	0.1	0.1	0.1	0.4	0.3	0.6	0.0	0.8	0.5	0.6	0.6	0.4
CB 114	0.1	0.0	0.0	0.2	0.0	0.1	0.0	0.0	0.0	0.0	0.0	0.0	0.0	0.0	0.0	0.0	0.0	0.0	0.0	0.0
CB 188	0.0	0.0	0.0	0.0	0.0	0.0	0.0	0.0	0.0	0.0	0.0	0.0	0.0	0.0	0.0	0.0	0.0	0.0	0.0	0.0
CB 153	0.8	0.2	0.3	1.5	0.0	1.1	0.2	0.0	0.1	0.0	0.2	0.4	0.1	0.2	0.0	0.9	0.5	1.0	0.7	0.3
CB 168 + CB105	1.2	0.3	0.5	2.7	0.0	1.6	0.1	0.0	0.1	0.0	0.1	0.3	0.2	0.4	0.0	0.4	0.3	0.3	0.4	0.2
CB 141	0.2	0.1	0.1	0.3	0.0	0.2	0.0	0.0	0.0	0.0	0.0	0.1	0.0	0.0	0.0	0.2	0.1	0.3	0.2	0.1
CB 137	0.0	0.0	0.0	0.1	0.0	0.0	0.0	0.0	0.0	0.0	0.0	0.0	0.0	0.0	0.0	0.0	0.0	0.0	0.0	0.0

CB 138	0.9	0.3	0.4	1.8	0.0	1.2	0.2	0.0	0.1	0.0	0.3	0.5	0.2	0.3	0.0	1.0	0.6	1.1	0.8	0.4
CB 158	0.1	0.0	0.0	0.2	0.0	0.1	0.0	0.0	0.0	0.0	0.0	0.0	0.0	0.0	0.0	0.1	0.0	0.1	0.1	0.0
CB 126	0.0	0.0	0.0	0.0	0.0	0.0	0.0	0.0	0.0	0.0	0.0	0.0	0.0	0.0	0.0	0.0	0.0	0.0	0.0	0.0
CB 178	0.0	0.0	0.0	0.1	0.0	0.0	0.0	0.0	0.0	0.0	0.0	0.0	0.0	0.0	0.0	0.0	0.0	0.1	0.0	0.0
CB 187	0.2	0.1	0.1	0.3	0.0	0.2	0.0	0.0	0.0	0.0	0.1	0.1	0.0	0.1	0.0	0.2	0.1	0.3	0.2	0.1
CB 183	0.1	0.0	0.0	0.1	0.0	0.1	0.0	0.0	0.0	0.0	0.0	0.0	0.0	0.0	0.0	0.1	0.1	0.2	0.1	0.1
CB 128	0.2	0.0	0.1	0.3	0.0	0.2	0.0	0.0	0.0	0.0	0.0	0.1	0.0	0.0	0.0	0.1	0.1	0.1	0.1	0.0
CB 167	0.0	0.0	0.0	0.1	0.0	0.1	0.0	0.0	0.0	0.0	0.0	0.0	0.0	0.0	0.0	0.0	0.0	0.0	0.0	0.0
CB 177	0.1	0.0	0.0	0.2	0.0	0.1	0.0	0.0	0.0	0.0	0.0	0.1	0.0	0.0	0.0	0.1	0.1	0.2	0.1	0.1
CB 171 + CB202	0.1	0.0	0.0	0.1	0.0	0.1	0.0	0.0	0.0	0.0	0.0	0.0	0.0	0.0	0.0	0.1	0.1	0.1	0.1	0.0
CB 156	0.1	0.0	0.0	0.1	0.0	0.1	0.0	0.0	0.0	0.0	0.0	0.0	0.0	0.0	0.0	0.1	0.0	0.1	0.1	0.0
CB 157 + CB201	0.0	0.0	0.0	0.0	0.0	0.0	0.0	0.0	0.0	0.0	0.0	0.0	0.0	0.0	0.0	0.0	0.0	0.0	0.0	0.0
CB 180	0.4	0.1	0.1	0.7	0.0	0.5	0.1	0.0	0.0	0.0	0.1	0.2	0.0	0.2	0.0	0.6	0.3	0.7	0.5	0.2

CB 193	0.0	0.0	0.0	0.0	0.0	0.0	0.0	0.0	0.0	0.0	0.0	0.0	0.0	0.0	0.0	0.0	0.0	0.0	0.0	0.0
CB 191	0.0	0.0	0.0	0.0	0.0	0.0	0.0	0.0	0.0	0.0	0.0	0.0	0.0	0.0	0.0	0.0	0.0	0.0	0.0	0.0
CB 169	0.0	0.0	0.0	0.0	0.0	0.0	0.0	0.0	0.0	0.0	0.0	0.0	0.0	0.0	0.0	0.0	0.0	0.0	0.0	0.0
CB 170	0.2	0.1	0.1	0.4	0.0	0.3	0.1	0.0	0.0	0.0	0.1	0.1	0.0	0.1	0.0	0.3	0.2	0.4	0.3	0.1
CB 199	0.1	0.0	0.0	0.1	0.0	0.1	0.0	0.0	0.0	0.0	0.0	0.0	0.0	0.0	0.0	0.1	0.0	0.1	0.1	0.0
CB 203	0.1	0.0	0.0	0.1	0.0	0.1	0.0	0.0	0.0	0.0	0.0	0.0	0.0	0.0	0.0	0.1	0.0	0.1	0.1	0.0
CB 189	0.0	0.0	0.0	0.0	0.0	0.0	0.0	0.0	0.0	0.0	0.0	0.0	0.0	0.0	0.0	0.0	0.0	0.0	0.0	0.0
CB 208 + CB195	0.0	0.0	0.0	0.0	0.0	0.0	0.0	0.0	0.0	0.0	0.0	0.0	0.0	0.0	0.0	0.0	0.0	0.0	0.0	0.0
CB 194	0.1	0.0	0.0	0.1	0.0	0.1	0.0	0.0	0.0	0.0	0.0	0.0	0.0	0.0	0.0	0.1	0.0	0.1	0.1	0.0
CB 205	0.0	0.0	0.0	0.0	0.0	0.0	0.0	0.0	0.0	0.0	0.0	0.0	0.0	0.0	0.0	0.0	0.0	0.0	0.0	0.0
CB 206	0.0	0.0	0.0	0.0	0.0	0.0	0.0	0.0	0.0	0.0	0.0	0.0	0.0	0.0	0.0	0.0	0.0	0.0	0.0	0.0
CB 209	0.0	0.0	0.0	0.0	0.0	0.0	0.0	0.0	0.0	0.0	0.0	0.0	0.0	0.0	0.0	0.0	0.0	0.0	0.0	0.0
Total	**52.5**	**13.7**	**23.0**	**135.8**	**0.6**	**75.8**	**5.3**	**0.6**	**3.0**	**1.5**	**4.0**	**8.9**	**7.9**	**16.2**	**0.2**	**24.9**	**17.2**	**20.9**	**19.1**	**11.9**

697
698

Table S3. OTU numbers by sample for each taxonomic marker

	P0					P1						P2					P3		P4		
	Z2 F5	Z2 B3	Z3/4 B5	Z2 B4	Z2 B5	Z3/4 B1	Z2 B2	Z3/4 B3	Z3/4 B3	Z2 F2	Z3/4 E5	Z3/4 B4	Z2 F3	Z3/4 E2	Z3/4 E3	Z3/4 E4	Z3/4 E1	Z2 F1	Z2 F4	Z2 B1	Total OTUs
OTUs 16S (*Bacteria*)	597	455	427	504	580	660	576	571	x	759	737	x	659	602	793	562	706	651	388	731	**1463** (>99%)
OTUs 16S (*Archaea*)	3	4	9	3	3	7	1	10	x	4	3	x	2	0	2	0	2	2	0	4	**14** (<1%)
OTUs 18S	161	209	119	141	x	259	197	x	172	269	292	x	294	220	319	229	243	340	180	306	**752**
OTUs ITS	217	164	113	231	223	253	227	190	198	299	313	185	277	137	234	158	163	281	172	254	**685**

Table S4. qPCR programs

	Prokaryotic 16S rRNA gene		Eukaryotic 18S rRNA gene		ITS Region		Cycles
Denaturating			95°C	10min			1
Amplification	95°C	30 sec	95°C	30 sec	95°C	30 sec	40
	63°C	1min	50°C	1min	57°C	45 sec	
	72°C	30 sec	72°C	30sec	72°C	1 mn 30 sec	
Melting point			95°C	5sec			1
			65 to 97°C	1min			
Cooling	40°C 10 sec						1

Figure S1. Rarefaction curves

Rarefaction curves for each sample were calculated for (A): prokaryotic dataset, (B): eukaryotic dataset and (C): fungal dataset.

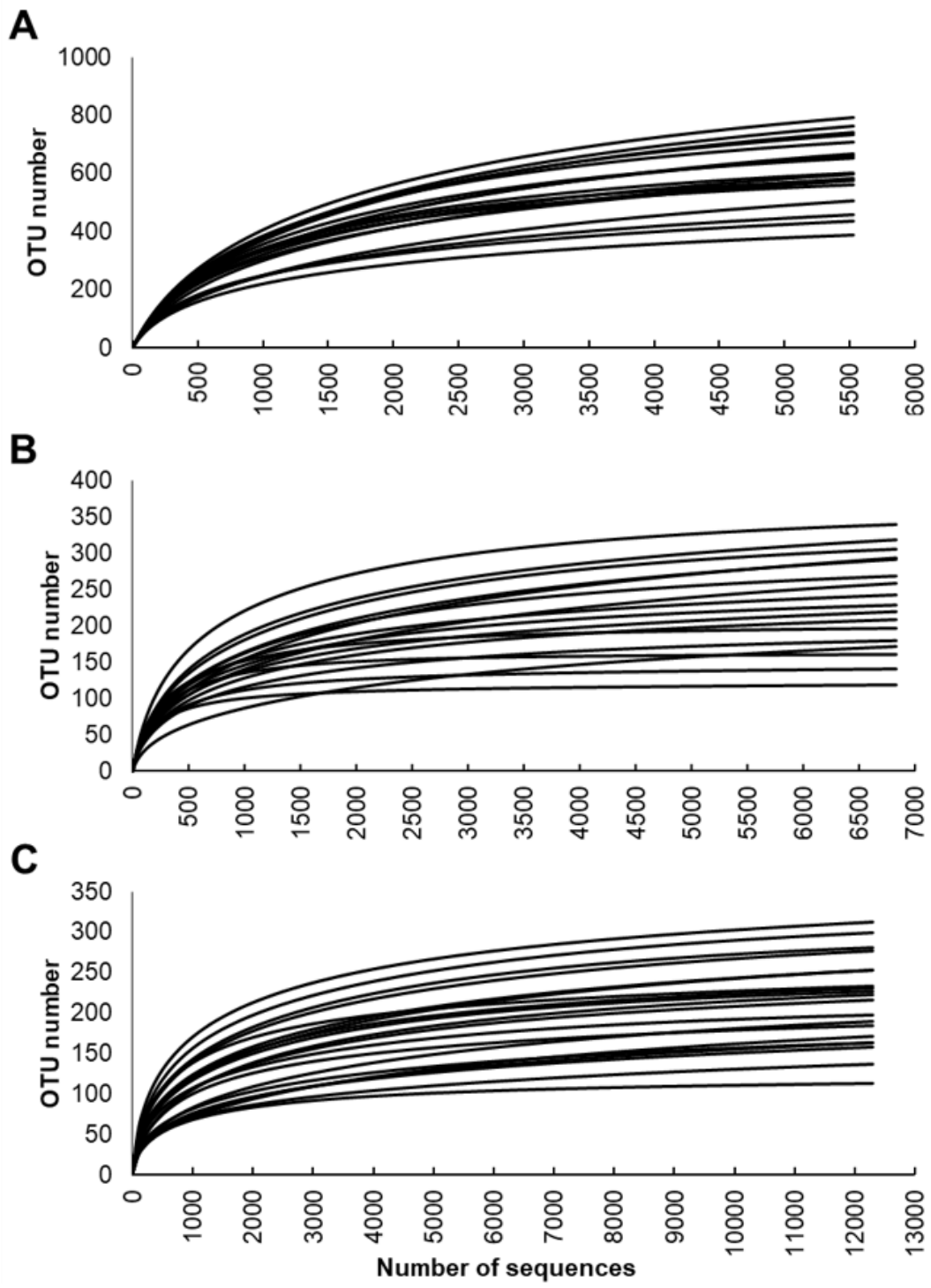

Figure S2. Alpha diversity indices

The richness and diversity indices (Chao1 and Shannon respectively) were calculated and illustrated by boxplots graphics for each group P0, P1, P2, P3 and P4 and with the following *pvalue* code (*) = ≥ 0.05 and ≤ 0.1 ; * = ≤ 0.05 ; ** = ≤ 0.01 ; *** = ≤ 0.001, for (**A**) : the prokaryotic dataset, (**B**) : the eukaryotic dataset and (**C**) : the fungal dataset.

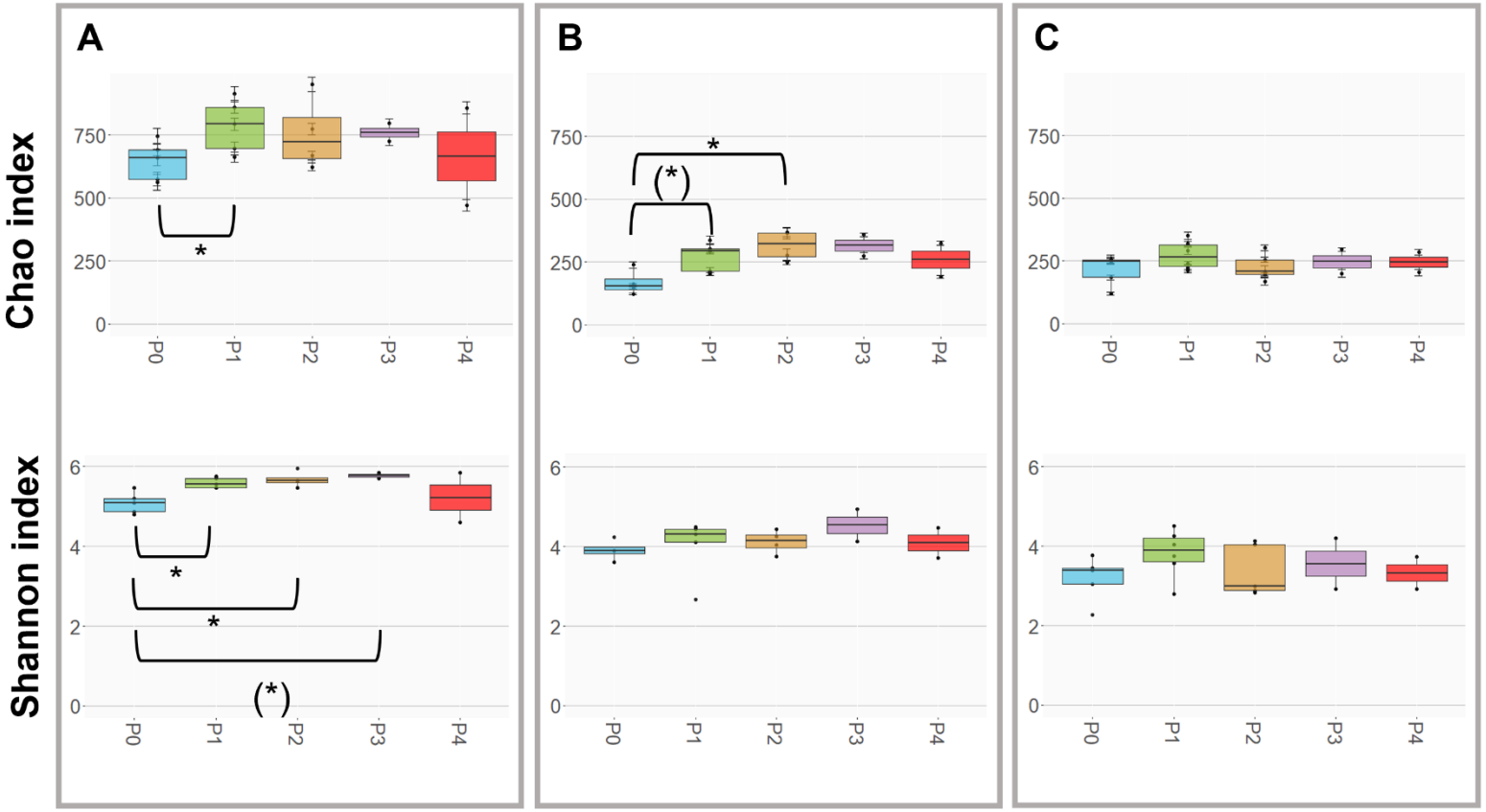

Figure S3. Venn diagram and bar diagram of prokaryotic dataset for OTU composition

At the top right corner, Venn diagram presented the shared and specific prokaryotic OTUs by sample group. Each bar diagram represented the number of OTUs by bacterial family for each sample group indicated in blue (P0), green (P1), orange (P2), purple (P3) and red (P4). The unknown families were not shown.

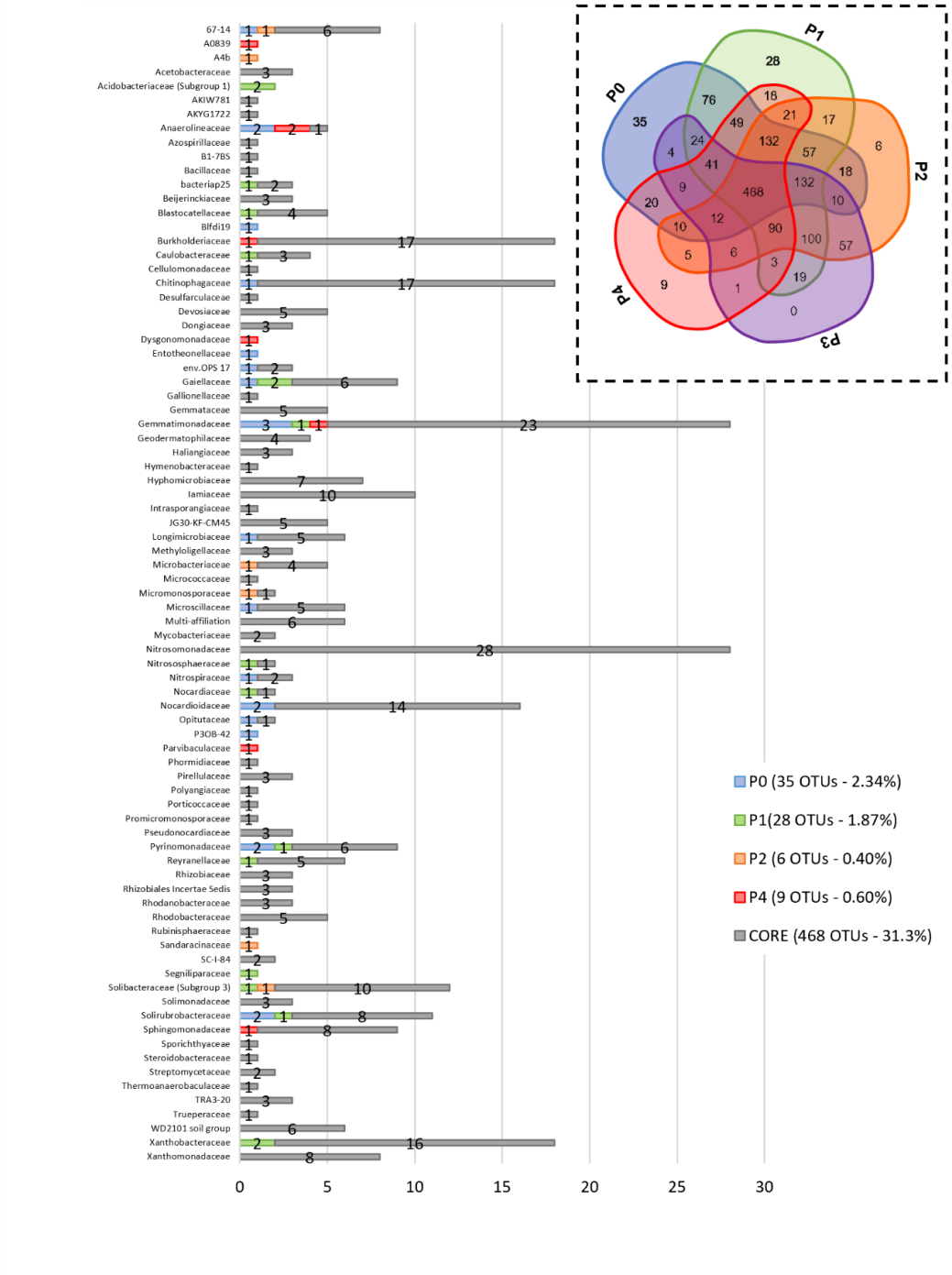

Figure S4. Venn diagram and bar diagram eukaryotic dataset for OTU composition

At the top right corner, Venn diagram presented the shared and specific OTUs by sample group. Each bar diagram represented the number of OTUs by eukaryotic family for each sample group indicated in blue (P0), green (P1), orange (P2), purple (P3) and red (P4). The unknown families were not shown.

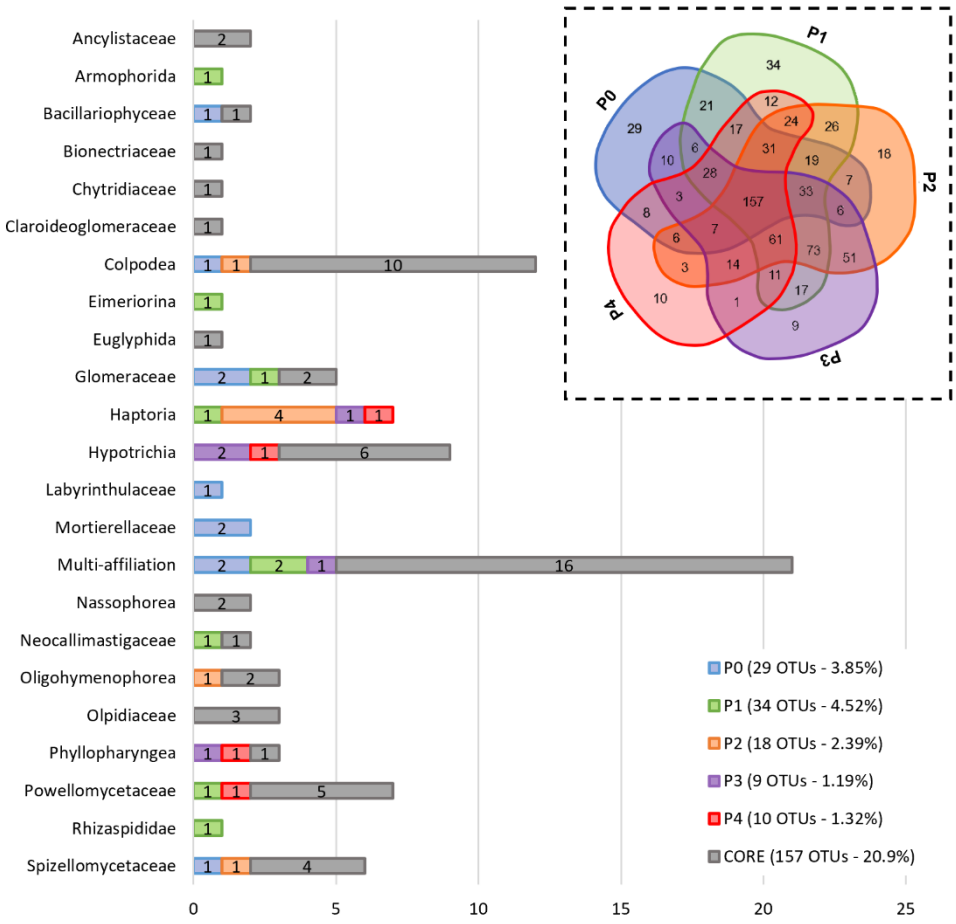

Figure S5. Venn diagram and bar diagram of fungal dataset for OTU composition

At the top right corner, Venn diagram presented the shared and specific OTUs by sample group. Each bar diagram represented the number of OTUs by fungal family for each sample group indicated in blue (P0), green (P1), orange (P2), purple (P3) and red (P4). The unknown families were not shown.

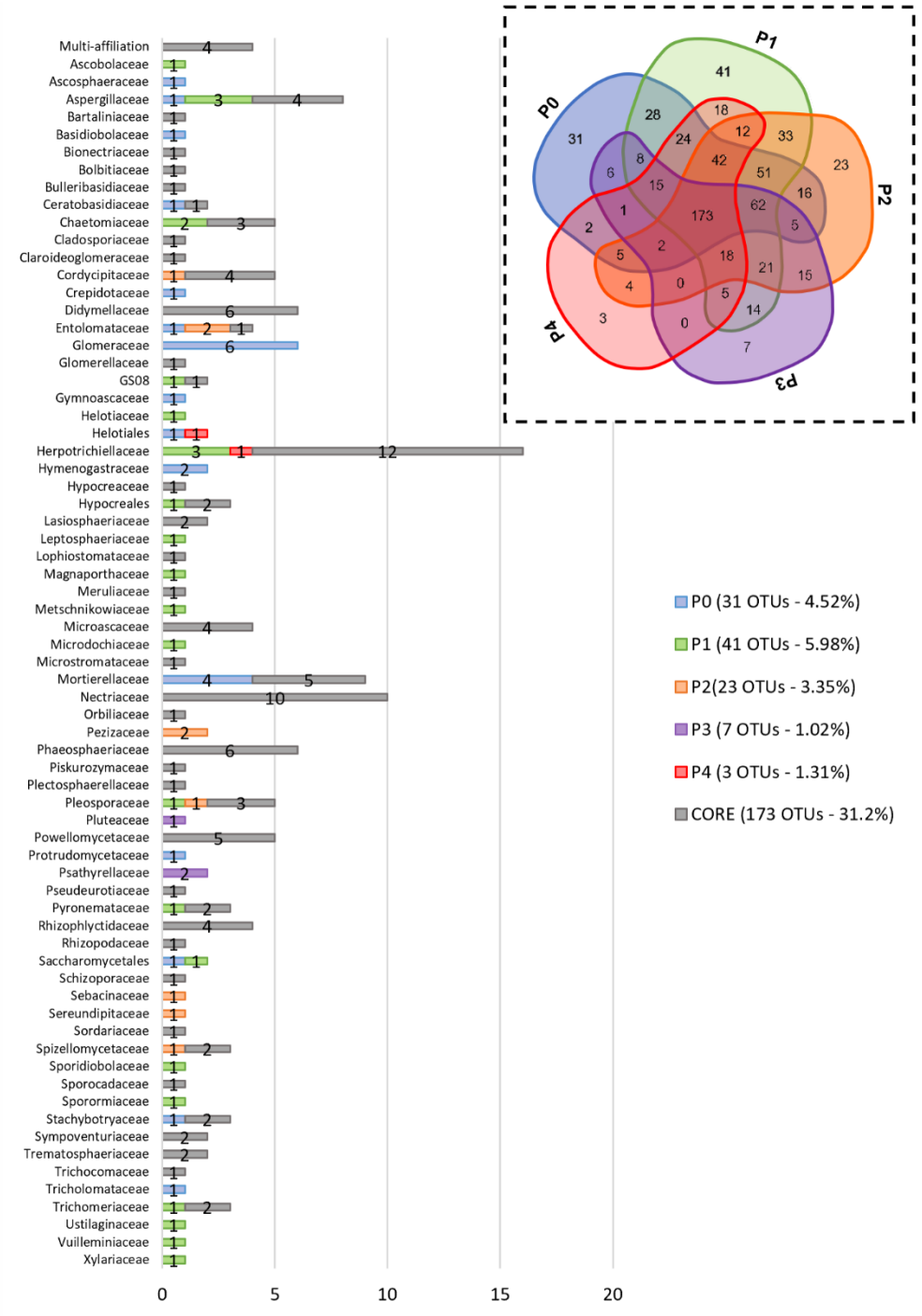

Figure S6. Abundance of the taxonomic marker sequences in the brownfield sampling site

The mean number of DNA sequence copies for (**A**): prokaryotic 16S rRNA, (**B**): eukaryotic 18S rRNA genes, (**C**): fungal ITS region were calculated for each group P0, P1, P2, P3 and P4 and with the following *pvalue* code (*) = ≥ 0.05 and ≤ 0.1 ; * ≤ 0.05 ; ** = ≤ 0.01 ; *** = ≤ 0.001

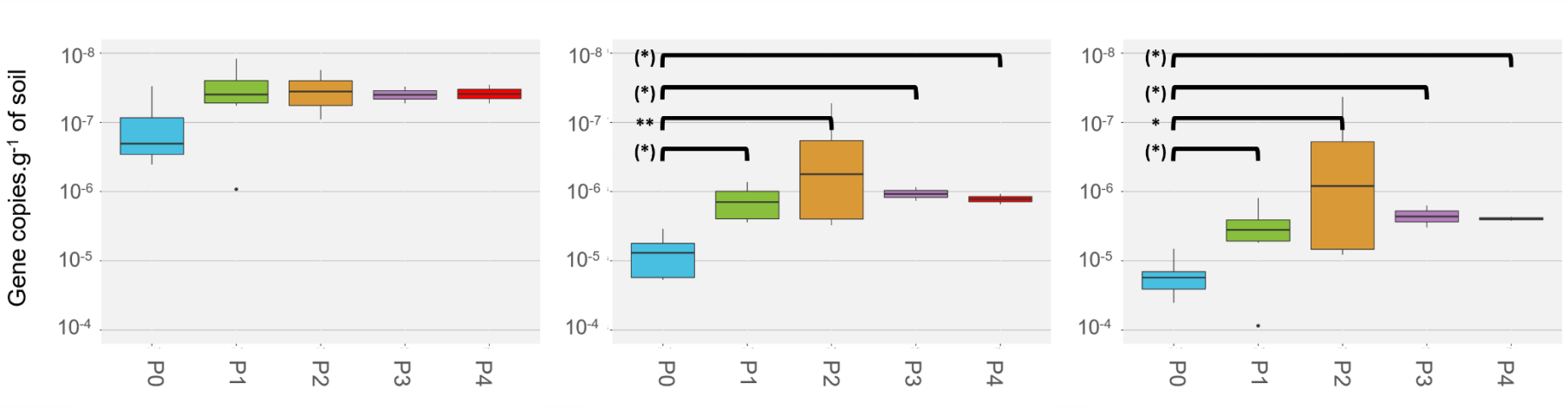

Figure S7. Total microbial activity kinetics

Total microbial activity was first (**A**) analyzed by mineralization kinetics expressed by µg of C-CO_2 by gram of dry weight of soil, assayed for each soil sample directly after sampling and appreciated by (**B**) FDA hydrolase enzymatic assay. Each pollution group P0, P1, P2, P3 or P4 were indicated by colors.